

THESIS ON NATURAL AND EXACT SCIENCES B30

Interaction of Humic Substances with Metal Cations

MONIKA ÜBNER

TUT
PRESS

Faculty of Science
Department of Chemistry
TALLINN UNIVERSITY OF TECHNOLOGY

Dissertation was accepted for the commencement of the degree of Doctor of Philosophy in Natural and Exact Sciences on September 27, 2004

Supervisor: Prof. Margus Lopp, Faculty of Science

Opponents: Prof. Dr. Toomas Tenno, University of Tartu, Estonia
Prof. Dr. Josef Havel, Masaryk University, Czech Republik

Commencement: November 30, 2004
Tallinn University of Technology

Declaration: Hereby I declare that this doctoral thesis, my original investigation and achievement, submitted for the doctoral degree at Tallinn University of Technology has not been submitted for any degree or examination.

/Monika Übner/

Copyright Monika Übner 2004
ISSN 1406-4723
ISBN 9985-59-479-7

Abstract

Humic substances (HS) are the product of microbial degradation, chemical polymerization and oxidation of organic matter. HS can be divided into different fractions: humic acid (HA), humatomelanic acid (HMA), fulvic acid (FA), and humin. While HS have many different functional groups then due to polyfunctionality, HS are the most powerful chelating agents among natural organic substances.

Estonia is rich in sea and lake sediments. Historically, those sediments have been used in human therapy as curative mud and those preparations may not contain organic and inorganic contaminants.

High molecular weight HS are an important part of sediments. The structure of HS from sediments in the Baltic region is not well studied. In the present work, the elementary composition of all soluble HS fractions and yield of HS from different sources was studied. The quantity of metal in the sediments and HS fractions was determined. As expected, HS from the sea sediment contain more metal than HS from the lake sediment. Differences in initial concentration of metals in HS fraction may reflect differences in their structure and show the metal binding ability and other properties.

Sedimentation experiments of metal/HS complexes showed that HA and HMA fractions have the best precipitation ability for heavy metals. The obtained results suggested that HA is more aliphatic than HMA. In lower heavy metal concentration, HMA has the best complexation properties.

Capillary electrophoresis, exactly the electrophoretically mediated microanalysis (EMMA) approach, was used for studying the interactions of HS with metal cations, using HS fractions as background electrolyte (BGE). HA, as a BGE without adding metal resulted in an electropherogram with a multiple number of spikes, the quantity of which is linearly correlated with the concentration of HA and with the applied voltage. It was found that other colloidal solutions also aggregate under high voltage. All HS fractions gave a different reproducible characteristic to each fraction electropherograms with metal ions, the shape of which is connected with the characteristic features of the structure of these fractions. The EMMA approach may be applied to study the interaction of HS with different compounds.

Humiinainete interaktsioonid metalli katioonidega

Kokkuvõte

Humiinained (HS) on orgaanilise aine mikrobiaalse lagunemise, keemilise polümeerisatsiooni ja oksüdatsiooni produktid. Humiinaineid võib fraktsioneerida järgmiselt: humiinhape (HA), hümatomelaanhape (HMA), fulvohape (FA) ja humiin. Kuna humiinained sisaldavad erinevaid funktsionaalseid rühmi, siis tänu sellisele polüfunktsionaalsusele kelaatuvad nad looduslikest orgaanilistest ühenditest kõige paremini.

Eesti on rikas mere- ja järvesetete poolest. Ajalooliselt on neid setteid kasutatud ravimudadena inimeste raviks ning sellised preparaadid ei tohi sisaldada orgaanilisi ja anorgaanilisi saasteaineid.

Setete oluliseks osaks on suure molekulmassiga humiinained. Balti regiooni setete humiinainete struktuuri on vähe uuritud. Käesolevas töös määrati erinevatest setetest eraldatud lahustuvate HS fraktsioonide elementaarkoostis ja saagis. Setetes ja saadud HS fraktsioonides määrati metallide sisaldus. Nagu võis arvata, sisaldavad meresette HS rohkem metalle kui järvesette HS. Algne metallide sisalduse erinevus humiinainete fraktsioonides võib peegeldada nende struktuurierinevusi ja näidata HS metallide sidumisvõimet ning teisi omadusi.

Metalli/humiinainete kompleksi sadenemise eksperimentid näitasid, et HA ja HMA sadenevad paremini koos raskemetallidega. Saadud tulemuste alusel võib oletada, et HA on rohkem alifaatne kui HMA. Madalatel raskemetalli kontsentratsioonidel komplekseerib metalle kõige paremini HMA.

Kapillaarelektroforeesi, nimelt selle elektroforeetilist mikroanalüüsi (EMMA) meetodit, kasutati HS ja metalli katioonide interaktsioonide uurimiseks, kasutades taustelektrolüüdina humiinained endid. Leiti, et HA ilma metalli lisamiseta annab rohkete piikidega elektroferogrammi, kus piikide arv korreleerub lineaarselt HA kontsentratsiooniga ja kasutatud elektrivälja pingega. Selliselt agregeeruvad kõrgepinge mõjul ka teised kolloidlahused. Kõik humiinainete fraktsioonid annavad EMMA meetodi kasutamisel metalli katioonidega igale fraktsioonile iseloomulikke reprodutseeritavaid elektroferogramme, mille kuju on seotud nende fraktsioonide struktuuriga. EMMA meetodit saab rakendada HS interaktsioonide uurimiseks erinevate ühenditega.

CONTENTS

1. LIST OF PUBLICATIONS.....	6
2. ABBREVIATIONS.....	7
3. REVIEW OF THE LITERATURE.....	8
3.1. Characterization of humic substances.....	8
3.2. Humic substances and capillary electrophoresis.....	10
3.3. Humic substances and metals.....	11
3.4. Interactions of metals with HS monitored by capillary electrophoresis....	15
4. AIMS OF THE STUDY.....	17
5. RESULTS AND DISCUSSION.....	18
5.1. Properties of HS fractions (Article I).....	18
5.1.1. Yield of the extraction of HS fractions from the sea and lake sediments.	18
5.1.2. Elementary composition of HS fractions.....	18
5.1.3. Metals in sediments and HS fractions.....	20
5.1.4. UV-VIS spectroscopy and calculated aromaticity.....	23
5.2. The precipitation ability of Zn^{2+} , Mg^{2+} , Mn^{2+} , Pb^{2+} , Cu^{2+} with different HS fractions (Article II).....	25
5.2.1. Effect of pH on the precipitation ability of Zn^{2+} /Sea HS complexes....	25
5.2.2. Precipitation of Zn^{2+} by HS fractions at pH 7.....	26
5.2.3. The precipitation ability of HA by different metals.....	28
5.2.4. Stability constants of precipitated metal/HS complexes.....	29
5.3. Capillary electrophoresis and HS (Article III).....	30
5.3.1. Flow of HA solution in capillary without applying electric field.....	31
5.3.2. Pumping HA solution with applying electric field.....	31
5.3.3. Comparison of the behaviour of cyclodextrin (CD) and HS solutions in the electric field.....	34
5.4. Interactions of Pb^{2+} and Zn^{2+} with HS by electrophoretically mediated on- capillary microanalysis.....	35
5.4.1. Interaction of Pb^{2+} with HS fractions (Article IV).....	36
5.4.1.1. Electropherograms of HS fractions.....	36
5.4.1.2. Hypothetical model of the process occurring in the capillary.....	37
5.4.1.3. Quantitative relationships of peak areas with added cation concentration.....	38
5.4.1.4. Comparison of complexes I and II.....	41
5.4.1.5. The rate of the formation of different complexes.....	42
5.4.2. Interactions of Zn^{2+} with HA.....	43
CONCLUSIONS.....	45
REFERENCES.....	46
ACKNOWLEDGEMENTS.....	57

1. LIST OF PUBLICATIONS

This thesis is based on the following articles referred to in the text by Roman numbers.

- I Übner, M., Treuman, M., Viitak, A., Lopp, M. Properties of humic substances from the Baltic Sea and Lake Ermistu Mud. *J. Soils Sediments* 2004, 4, 24-29.
- II Übner, M., Treumann, M., Viitak, A., Lopp, M. The interaction of metal cations with different humic substances from sediments of the sea and lake. *Proc. Estonian Acad. Sci. Chem.*, 2005, 54, 24-34.
- III Übner, M., Lepane, V., Lopp, M., Kaljurand, M. Electrophoretic aggregation of humic acid. *J. Chromatogr. A* 2004, 1045, 253-258.
- IV Übner, M., Kaljurand, M., Lopp, M. Interactions of Pb^{2+} with fulvic acid by electrophoretically mediated on-capillary microanalysis. *J. Chromatogr. A* 2004, 1057, 253-256.

2. ABBREVIATIONS

Ac.lake FA	fulvic acid from the acid pre-treated LM
Ac.lake HA	humic acid from the acid pre-treated LM
Ac.lake HMA	hymatomelanic acid from the acid pre-treated LM
Ac.LM	the acid pre-treated LM
Ac.sea FA	fulvic acid from the acid pre-treated SM
Ac.sea HA	humic acid from the acid pre-treated SM
Ac.sea HMA	hymatomelanic acid from the acid pre-treated SM
Ac.SM	the acid pre-treated SM
BGE	background electrolyte
CD	cyclodextrin
CE	capillary electrophoresis
EMMA	electrophoretically mediated microanalysis
EOF	electroosmotic flow
FA	fulvic acid
HA	humic acid
HMA	hymatomelanic acid
HS	humic substances
Lake FA	fulvic acid from the LM
Lake HA	humic acid from the LM
Lake HMA	hymatomelanic acid from the LM
LM	sediment of Lake Ermistu
Sea FA	fulvic acid from the SM
Sea HA	humic acid from the SM
Sea HMA	hymatomelanic acid from the SM
SM	sediment of the Baltic Sea
UV-VIS	ultraviolet-visible

3. REVIEW OF THE LITERATURE

3.1. Characterization of humic substances

Humic substances (HS) are found in soil, peat, coal, water, sediments, and other natural materials as a product of biological and chemical processes of transforming organic matter [1,2,3]. HS play a fundamental role in the accumulation and exchange processes of chemical compounds (metals and organic pollutants) in the environment [2]. HS are believed to be complex heterogeneous and polydisperse mixtures of nonstoichiometric composition [4]. HS constitute an important reservoir of organic carbon in the aquatic and terrestrial ecosystem [5].

HS are formed through aerobic and anaerobic decomposition of plants, as well as by secondary microbial synthesis. Differences in origin, age, and genesis (existence of an enormous number of different precursor materials) lead to a high degree of chemical and morphological complexity of the matter that makes the HS difficult to characterize and thus, the exact structure of HS cannot be defined [6]. The proposed hypothetical structures are based on the knowledge obtained from the studies of elemental composition, functional group content, degradation products, spectroscopic data, and physical-chemical properties of HS [7-9]. In general, HS can be defined by combining all the known aspects of their properties, including the process of their isolation [10].

HS are largely composed of a self-assembly of molecules which give pseudo-high molecular weight properties to the complex [11]. The conformation of the humic material in a neutral solution is stabilised predominantly by weak intermolecular hydrophobic forces, which hold together smaller humic subunits in apparently large molecular dimensions. HS behave in solution as associations of small molecules held together mainly by hydrophobic forces rather than as macromolecular random coils [12].

The classical fractionation of HS is based on solubility differences at different pH values. According to that, HS are defined as highly transformed amorphous dark coloured materials that can be divided into four fractions: 1) humic acid (HA) – soluble in water at higher pH values; 2) humatomelanic acid (HMA) – soluble in ethanol; 3) fulvic acid (FA) – soluble in water under all pH conditions; 4) humin – not soluble in water at any pH value. HS sorb many biological molecules like peptides, sugars, nucleic acid residues, and fats [1,7,13]. The free HS are directly soluble in alkali, while the bound HS have to be treated with HCl or some other acid in order to convert them from calcium and magnesium salts into free acids that dissolve in alkali [14].

The most common functional groups of HS include hydroxyl groups of phenols and alcohols, carbonyl groups of ketones/quinones, aldehydes, carboxylic groups, amino- and nitro-groups, and sulphur containing entities from thiols, sulfates and sulfonates [4,6,7]. In general, it is accepted that HS contain different classes of compounds like hydrocarbones (including arenes), carbohydrates, peptides, terpenes, etc.

In FA, the amount of carboxylic and phenolic groups is higher than for HA [2,6,15]. HA from aqueous systems is less aromatic and more highly oxidized than that from soils [11]. The content of carboxylic and phenolic groups in sedimentary HA is usually lower than observed for soil and water HA, while carbonyl content is higher [16]. In the literature, data about the functional groups of HMA are scarce. Besides those major functional groups cited above, HMA contains also different subunits from fatty acids, waxes, carbohydrates, terpenes, and nitrogen containing compounds [17,18].

HS may also contain carbohydrates, which are bound to the central core through H-bonding only. Those complex polysaccharides are known to have an ability to bind inorganic soil particles into a stable aggregate [7,11]. In soil HA, the most common monosaccharides are glucose and mannose. More carbohydrates are found in FA than in HA [19]. It has been suggested that galactose, mannose, and rhamnose are primarily of microbial origin, while arabinose and xylose are predominantly plant derived and glucose originates from both plants and microorganisms [20]. Carbohydrates and proteinaceous materials are adsorbed on outer HS surfaces and in internal voids. It is likely that hydrogen bonding is also involved in these interactions [21]. Aquatic HS have significantly less carbohydrates and amino acids than soil HS. In aquatic HA, their content is especially low [11].

In water solutions of HS fractions (especially HA) they behave as supramolecules that are able to polymerize (oligomerize), aggregate, form micelles and form supramolecular ensembles with other compounds [22-25]. Like a micelle, HA has a hydrophobic interior and more hydrophilic surface. These structures have been referred to be pseudomicelles. It is likely that intermolecular aggregation supplements, intramolecular coiling in the formation of pseudomicelles, and that depends on both, the concentration and the polydispersity of the solute [6]. HA molecules are supposed to consist of long flexible polymers, which have a tendency to coil up and aggregate. This process depends largely on the pH of the solution and on the hydrophobic interactions that exist between polymer chains. Aggregation is supported by functional groups bridging and combined charge neutralization [24,26]. The mutual repulsion of carboxyl and hydroxyl groups causes the HA polymers to adopt a stretched configuration. All HA solutions are polydisperse and the interaction of segments of different sizes might lead to a different degree of intermolecular interactions that further increase the formation of supramolecules and their aggregation [24]. HAs from different sources aggregate differently: highly solvated HAs aggregate poorly, while a lignite derived material (soil HAs) undergo intermolecular rather than intramolecular, rearrangements. A newly discovered algal HA was found to have minimal aggregative properties [25]. Small FA molecules show less evidence of aggregation at low concentrations [26,27].

Thus, it can be concluded that distinct compositional differences exist between HS from different sources (from different types of soils and climate zones). In order to understand the major processes and mechanisms that occur

in soil and in water, it is obligatory to know the components of HS [1] and to compare their behaviour in aqueous solution in order to understand how their environmental interactions may differ from each other [25].

3.2. Humic substances and capillary electrophoresis

In recent years, many different analytical approaches have been used to isolate HS, to fractionate them before further investigation, and to obtain information about their structure and properties [28]: ultrafiltration [29,30]; elemental analysis [31-34]; IR-spectroscopy [31-33,35-38]; ¹³C-nuclear magnetic resonance spectroscopy [31,32,34,35,37-41]; UV/VIS spectroscopy [34,36-38]; size exclusion chromatography [34,42-44]; fluorescence spectroscopy [35,36,38,45,46]; electron paramagnetic resonance spectroscopy [35,38]; gas and liquid chromatography [47-51]; electrospray ionization mass spectrometry [52,53]; conductometric characterization [54].

Capillary electrophoresis (CE) is one of the recent methods for the characterization of HS [8,22,24,28,55-61]. CE allows miniaturization and automation of the classical electrophoretic methods into an effective and rapid method with only a minimal amount of sample. After filling the fused silica capillary with the buffer (microliters) and loading the sample (nanoliters) on the anode side, the voltage is applied. The quartz capillary wall is negatively charged (ionization of the silanol groups as a function of pH) and attracts positively charged ions from the buffer, creating an electrical double layer. With the presence of the voltage across the capillary, the cations of the double layer migrate to the cathode, creating a net flow of buffer solution to the negative electrode (electroosmotic flow – EOF) [62,63].

CE combines the unique possibility to separate and detect natural organic matter in aqueous solution within a wide pH range, i.e., close to the environmental conditions, and to obtain information on their charge density (electrophoretic mobility being governed by charge and size). Dissolved HS at pH 7 carry a negative charge because practically all acidic carboxylic groups of humic solutes are deprotonated (negatively charged) [26,59]. The presence of negative charge permits, using uncoated capillaries, to separate HS solutes by electrophoresis in an electrical field with polarity (+) → (–) in which EOF is responsible for the movement of solutes [59]. HS electropherograms consist of broad shaped peaks that can be called humic “humps”, which sometimes have shoulders. It is generally suggested that the “hump” corresponds to the average electrophoretic mobility of a HA mixture [22]. In general, on the electropherograms of HA, two (or sometimes multiple) “humps” are observed [4,57,64]. Frequently, on these “humps”, multiple randomly scattered sharp peaks (“spikes”) appear (see e.g. electropherograms in [8,22,55,57,58,65]). The difficulties in the interpretation of the obtained signals of HS with any of the described analytical approaches arise from the high polydispersity in the structure of these materials [4,55]. CE measurements have confirmed the micellar properties of HS. Schmitt et al. [66] determined the concentration at

which the HS associates behave like ionic micelles. Those micellar associates are probably responsible for the aggregation of the HA molecules. HS cluster into aggregates and because of the polydisperse nature of the aggregates, the electrophoretic mobility in a free solution is not sufficient to achieve separation [55].

Usually, the formation of spikes in CE is associated with air bubbles in the buffer and considered as artefacts that do not induce scientific interest. It has also been suggested that the spikes correspond to some specific compounds present in all HA, which are liberated from the supramolecular structure of the HA by the action of different buffer constituents (e.g. boric acid [8,22,24,56,67], phosphate [22], cyclodextrins (CD)[57]). In addition, it has been proposed that the “spikes” obtained with boric acid buffer represent individual monomeric fragments of HA [24] or the presence of aggregates in the unfiltered buffer solutions [4]. Recent studies of CE of bacteria associate spikes unanimously with the formation of aggregates in the CE buffer under the applied voltage. It was demonstrated by the visual observation of the process of clustering of the scattered individual fluorescing bacteria into a large aggregate, using the illumination of the whole separation space in capillary by laser [68,69]. However, bacterial aggregates provide good insight to understanding the aggregation phenomenon in the electric field. First, the appearance of spikes on electropherograms indicates (as one cause) the presence of aggregates. Second, the addition of some components (like imidazole) into HA solution presumably changes surface chemistry (like polyethylene oxide in the case of bacterial solutions [68,69]). Usually, the observed spikes are considered artefacts and are usually neglected. The nature of spikes in HA electropherograms is not always well explained.

3.3. Humic substances and metals

The ability of HS to react with cations has long been recognized because of strong association of HS with organic and inorganic compounds in soil and water, acting as both storage and transport agents for these species [6]. Due to the polyfunctionality of HS, they have a strong affinity toward metal cations and therefore can interact strongly with various metal ions to form HS complexes and affect the adsorption/desorption behaviour of metals [4,7,9,23,70,71,72]. The mobility and transport of metal ions in the environment is strongly influenced by their complexation with HS [6,9,73-75]. HS have a great potential for reactivity with many natural and anthropogenic chemicals [5]. Information about the content of metals in HS is useful for better understanding of mobilization and transport mechanisms of trace metals for environmental remediation efforts and soil nutrition studies, as well as their toxicity and bioavailability [76,77]. The migration behaviour of metallic elements in natural ecosystems is of particular importance because of severe problems of environmental pollution [70]. Lately, adsorption of metal ions on the HS of various origins was studied [78-83].

HS are widespread constituents of natural environment. It is known that the addition of cations, especially metals, to a HS solution changes the intramolecular forces and HS molecules have a tendency to coil up with relatively hydrophobic interiors and hydrophilic surfaces. Also, the formation of aggregates is highly metal dependent [6,84]. Due to the size changes induced by conformational rearrangement and aggregation/dissociation arising from intermolecular hydrogen bonding, HS can form soluble complexes that can migrate long distances or precipitate, carrying bound cations with them. The migration/precipitation abilities depend on the metallic ion, the cation charge, the degree of ionization of the organic molecule, the ionic strength of the media, and the location of the metal ion [85].

Aggregation processes depend strongly on the structure and nature of the HS and their metal complexes [26,86]. The presence of metal cations inevitably leads to further interactions that usually result in the formation of a visible colloid and eventual flocculation at sufficiently high ionic strengths [26,27]. HS are highly penetrated by solvent molecules and small ions. As metal concentration increases, larger organic moieties are removed from the solution by precipitation. Aggregation experiments, even at higher metal concentrations, revealed that some low weight HS always remains in solution. The addition of metals could cause colloidal instability and aggregation by two possible mechanism [86]:

1. The increased cation concentration is causing a compression of the colloidal double layer, reducing the inter-molecular repulsion;
2. The metals are forming chemical bonds with the functional groups in the HS structure, neutralizing the HS charge and hence the inter-molecular repulsion. The charge neutralizing of the HS that accompanies specific metal binding is responsible for aggregation.

In the slightly alkaline HS solution, the humic molecules are polyanionic and have a slight tendency to aggregate in either an inter- or intramolecular fashion. The addition of metal ion to HS results in charge neutralization and bridging of carboxyl groups on different sections. These chains are drawn together, forming a micelle-like structure [27].

The added metals do not only promote aggregation but also produce a more hydrophobic structure that may further enhance the tendency for flocculation by increasing the attractive forces between HS molecules. The aggregation takes place immediately before precipitation while flocculation requires some time [5,86].

It has been suggested that the role of metal ions in HS interactions may be both intramolecular and intermolecular [6,26]. HS solutions flocculate when the ionic strength is raised. The flocculation of the HS with metal cations is due to increased intramolecular bonding and folding of the macromolecules. The higher molecular weight fractions precipitate from the solution first, because larger molecules are more sensitive to changes in inter- and intramolecular interactions upon reactions with the metals. Dissolved HS molecules bear significant negative charges, which prevent both the intra- and intermolecular

association. Partial neutralization by cationic species in the solution allows coiling and folding of the polymer [5,6]. The metal ions brought into contact with HS first occupy binding sites in the outer sphere of HS macromolecules and the less accessible binding sites in the inner sphere of the macromolecules are reached later [77]. Thus, only after all carboxyl groups and part of the phenolic groups of the HS are involved in complexation with metal, insoluble complexes begin to precipitate from the solution [5].

On the other hand metal binding to HS fraction affords information about the structure of the HS and about of the differences of the HS fractions. The type of metal ion, solution concentration and molecular size of HS fractions affect stability of metal/HS complex [87]. It is suggested that HS have as a minimum two different binding sites for metal cations. The first site represents nitrogen and sulphur bearing functional groups. These groups give the strongest metal binding sites and they consist of a very large number of site types. The main process is an exchange of Na^+ by M^{2+} . This mode of complexation is not much affected by pH. The largest number of functional groups – oxygen functionalities, represents the second binding site for metal cations. This mode of metal-ion complexation is dependent on pH [87-90]. As the metal/HS ratio is increased, the metal ions first complex at those sites to which they are most suited (the strong binding sites). Then, as these are saturated, they enter the sites for which they have a lower affinity (weaker binding sites) [90,91]. Carboxylic groups in HS are not binding all inserted metal ions. Many of these groups are probably hidden and inaccessible for metal ions in the macromolecular matrix of HS [75].

In the literature, only studies of metal/HS complexes for HA and FA fractions can be found. The ability of HA to bind metals depends strongly on the pH. The maximum metal sorption capacity was achieved in a neutral or slightly acidic medium. More strongly bound metals push less strongly bound ones out [89]. The sources of HA and the extraction or isolation procedure, concentration of HA, pH and method of analysis of the complex may affect the stability constant of the complexes [92]. The stability constant order for different metal/HA complexes differs slightly, and was found to be $\text{Pb} > \text{Cu} > \text{Zn} \sim \text{Mn} > \text{Mg}$ [89]; $\text{Cu} > \text{Pb} > \text{Zn} > \text{Mn} > \text{Mg}$ [92]; $\text{Pb} > \text{Cu} > \text{Zn} > \text{Mn} \geq \text{Mg}$ [93]; $\text{Pb} > \text{Cu} > \text{Zn}$ [16]; $\text{Pb} > \text{Cu} > \text{Mn} > \text{Zn} > \text{Mg}$ [81]. Each cation is bound to HS in its own way [78]. The atomic weights of the metals play a critical role [81].

Reactions of HA with metal ions were found to occur in two ways: a major one, in which both acidic carboxyls and phenolic hydroxyls participate simultaneously and a minor one, in which only the acidic carboxyls are involved. The addition of any metal ion leads to the interactions of those with negatively charged moieties on the HA chains (especially COO^-). HA configuration changes with the involvement of relatively stable inner sphere [92]. Among the HS fractions, FA has greater affinity towards metal ions because they contain a relatively high amount of oxygen functionalities (carboxylic and phenolic groups) [94].

It is known that HA and FA have higher affinity for Pb^{2+} and Cu^{2+} [15,74,76,80,81,83,89,94-96] and they form at least two different types of complexes. Those metals bind to carboxyl and hydroxyl structures and nitrogen containing moieties [15,16,78,81,91]. IR spectra of the metal/HA complexes show that Pb^{2+} and Cu^{2+} react with carboxylic and phenolic groups as well. The higher pH of the solution, the higher is the adsorption ability of the ions [81]. As Cu^{2+} and Pb^{2+} ions exhibit a stronger affinity to the carboxylic groups of HS [97,98], those metals prevail to form inner sphere complexes with O-containing functional ligands at pH 6 [97,99]. FA contains a variety of sites with variable ability to complexate metal ions. It has been found that Pb^{2+} /FA complex begins to precipitate before the FA complexing capacity for the metal ion has been reached [96]. At low to moderate metal ion concentrations, Cu^{2+} is bound more strongly to the HS than Pb^{2+} . Only at higher free metal concentrations, the amounts of metal ions sorbed were larger for Pb^{2+} than for Cu^{2+} [100].

HA and FA from various origins are similar in their metal ion adsorption properties and shows a similar amount of available binding sites (complexation capacity). Thus, heavy metals bind to the same reaction site present in HA or FA [81,91,94,101]. At the same time, Jerzykiewicz [102] has found that the interaction of HA with Pb^{2+} ions results in the formation of radicals the concentration of which depends on the Pb^{2+} content in the complex. Those radicals are typical of aromatic condensed structures around the metal ion.

Binding experiment with Suwannee River FA and divalent metal cations (Pb^{2+} , Mg^{2+} , Zn^{2+}) showed that the major characteristic of FA is the flexibility of the carboxylic groups. This flexibility allows for the binding of ions of different ionic radii with minor accompanying variations in the molecular structure [103].

Zn^{2+} has a different binding structure in different HS fractions. In aquatic FA and HA, Zn^{2+} tends to complex with O-containing functional groups (carboxyl and hydroxyl). In soil HS, Zn^{2+} tends to complex with thiol and amino groups [74,91,104,105]. The Zn^{2+} binding with HA in the pH range 3 – 6.5 is only 30%. That indicates to the formation of weak complexes with HA [16,74,76,91].

Mn^{2+} is chelating in a five- or six-membered ring structure, or in highly ionic species, perhaps reflecting carboxylate salt formation [91,104].

Mg^{2+} is typically reacting readily with acidic organic groups, of which carboxylic groups are the most obvious [91]. Mg^{2+} /HA complexes may include a large amount of hydrating water [81].

Many authors use lyophilized HS for making the HS solution. Lyophilization may change the molecular structure of HS that never recovers. Martyniuk and Wieckowska [81] have found that the metal adsorption on HA gel was slightly higher than adsorption on the respective solid HA sample. Thus, in the investigation of metal/HS complexation, the non-lyophilized HS fractions are preferred.

3.4. Interactions of metals with HS monitored by capillary electrophoresis

Extensive research has focused on the metal-binding properties of HS. As most of the methods are based on distinguishing between “free” and HS-bound metal, separation methods are widely employed. Numerous studies of metal/HS interactions use many different analytical methods [106]: size exclusion chromatography [73], fluorescence spectroscopy [74,94,107], potentiometric titration [16,72,78]; stripping chronopotentiometry [108]; capillary electrophoresis [5,23,59,77,78,101,109]; ultracentrifugation and ultrafiltration [73,86,110]; column arrangement [70,92,93]; inductively-coupled plasma mass spectrometry [90,111]; X-ray absorption spectroscopy [97,105]; X-ray spectromicroscopy [112]; ion-selective electrodes [96,100]; Fourier transform infrared spectroscopy [98,102]; anodic stripping voltammetry [99]; conductivity measurements [26]; atomic emission spectrometry [80]; atom absorption spectroscopy [113]; polarographic methods [114,115].

CE has been generally recognized as a useful method in the area of metal analysis [5,77,101,109,116-122]. The separation principle of CE is based on the differential electrophoretic mobility of the charged compounds. The mobility of metal cations toward the cathode can be selectively moderated due to their partial complexation within the capillary, followed by the formation of metal complexes of different stability and thereby an effective charge [116,123]. To enhance selectivity (to provide a greater difference in electrophoretic mobility), addition of a complexing reagent to the background electrolyte to form metal complexes has been proposed. Complexing agent has to be able to form stable, negatively charged complexes with a great number of metal ions and must be suitable for a sensitive detection of analyte ions. Carboxylic acids as the complexing reagents are used for on-column complexation [121].

Two different approaches are used in CE for studying interactions of metal ions:

1. On-column complexation, where a soluble ligand is present in the running electrolyte and weak complexes are rapidly formed [117,118,121,122].
2. Pre-column complexation, where a strong ligand is added to the sample to form complexes before CE analyses [124,125].

In recent years, reactions inside capillary with their simultaneous electrophoretic separation have gained attention. This approach is especially popular among investigators interested in the kinetics of enzymatic reactions (after following the pioneering paper by Bao and Regnier [126]). That method is known as electrophoretically mediated microanalysis (EMMA) and is developed further by different researchers [127-129]. Recent publications give exhaustive overview of the present status of the EMMA method [130,131]. Besides enzymatic catalysis, EMMA is also used in complexation of metals with resorcinol [122]; in reactions catalyzed by transition metals [132], and in determination of Co^{2+} [133].

According to the EMMA approach, the reactants are introduced into the capillary inlet (to the background electrolyte) as separate bands. Upon application of an electric field, the two bands merge due to the differences of their electrophoretic mobilities. When chemical reaction occurs, the resulting products migrate away from the reaction zone and separate. Thus, the detector can individually determine the quantities of nonreacted substrate and products. Since the contact time of the reactants depends on the mobility differences of the reactant/product mixture as well as from the background buffer electroosmosis flow rate, its exact control and manipulation is problematic. Also, by rough estimation, the contact time is about ten seconds, which might be too short for slow reactions, and the amount of the product accumulated during the contact time might be too small to detect [131].

Using the EMMA approach, we can analyze the on-column complexation of metal and different HS fractions by CE, using HS as complexing agents. It is known that the mobility of metal cations toward the cathode can be selectively moderated due to the complexation within the capillary, followed by the formation of metal complexes of different stability and thereby effective charge [121,123]. This implies that the electrophoretic mobility of the negatively charged HS species is smaller than that of the EOF of the solution. The presence of metal ions changes the net charge of the HS and, consequently, its electrophoretic properties [77]. The mobility of all metals is reduced by the presence of the HS [26].

4. AIMS OF THE STUDY

HS were extracted from the sediments that have been used in Estonia as curative mud in human therapy for more than a century. Still, there is very little information of the HS and their fractions of the used sediments. In particular, the properties of the HMA fraction were of interest because of almost lack of information about it: HMA is not often extracted from the HS. There was not any information about metal ion complexation with HMA. Taking into account the polyfunctionality of HS, the metal complexation with HS fractions may give information about the structure of different HS fractions and HS in general. CE, especially the EMMA approach, may give new insight into the metal/HS binding. Polydisperse polycarboxylic acids like HS may form sufficiently stable and always negatively charged chelates with many different metal ions. Thus, they can be used as BGE in the CE analysis.

Therefore, the aims of the study are the following:

- To characterize and compare soluble HS fractions isolated from the sediments of the Baltic Sea and Lake Ermistu.
- To elucidate the metal content of the HS fractions.
- To study the specific precipitation of metals (Zn^{2+} , Mg^{2+} , Mn^{2+} , Pb^{2+} , Cu^{2+}) with different HS fractions.
- To investigate the interaction of the metal ions with HS fraction by CE using HS fractions as BGE (the EMMA approach).
- To apply the complexation data for the characterization of HS fractions.

5. RESULTS AND DISCUSSION

5.1. Properties of HS fractions (Article I)

5.1.1. Yield of the extraction of HS fractions from the sea and lake sediments

Sediments of sea and lake contain a great variety of organic compounds. Among them, HS play an important role. HA is the major component in HS fractions [2]. We determined the yield of basic extraction of different soluble HS fractions in the course of separation from sea and lake sediments (SM and LM, correspondingly) (Table 1) (Article I).

Table 1. Yield of the extraction of HS fractions from sediment g/kg of sediment dry weight

HS	SM	Ac.SM	LM	Ac.LM
HA	1.5	4.3	28.1	70.6
HMA	0.8	2.8	3.4	4.8
FA	2.4	1.4	2.3	3.6

The yield of the extraction of HS from LM and SM differs considerably: approximately six times more HS were extracted from LM than from SM. In the LM, the HA fraction dominates, while in the SM, the FA fraction prevails. The ratio of HS fractions (HA/HMA/FA) in the SM was 1.9/1.0/3.0 and in the LM, it was 8.3/1.0/0.7. The amount of FA in both sediments is almost equal.

Acid pre-treatment of both sediments (Ac.SM and Ac.LM, correspondingly) increased the amount of extracted HS. In the case of Ac.SM, the amount of HA increased by 2.9 times, HMA increased by 3.5 times but FA diminished by 0.6 times. In the Ac.LM, the amount of HA increased by 2.5 times, HMA increased by 1.4 times and FA, as different from the SM, increased by 1.6 times. These results demonstrate that SM and LM are quite different in respect to HS. This is obviously due to differences in SM and LM genesis. HS that are bound to the inorganic/organic structure of sediment are released in the course of prolonged treatment with acid. That result is in good accordance with the earlier findings [134].

5.1.2. Elementary composition of HS fractions

We performed elemental analysis of different HS fractions. The obtained results together with the atomic ratio and organic matter content of the different HS fractions are presented in Table 2.

In general, the elemental composition of HS was quite similar in all the studied fractions, although there were significant differences between the Sea and Lake HA. Sea HA had more nitrogen and Lake HA had more oxygen. The literature data [2,10] have revealed that carbon content in HA is higher than in FA and that FA contains more oxygen than HA [90]. Our results are in good

accordance with their findings for Sea HA and FA. We also separated HMA from HA and found that HMA had the highest carbon content and the lowest nitrogen content. These values are comparable with those found by Glebova [18] and Ilomets et al. [14]. The highest carbon content indicates the highest aromaticity (percentage of condensed structures) of HMA. This result is supported by a calculated aromaticity of the samples (Table 5). The oxygen content of HS indicates that Lake HA contains more heterocyclic structures as well as carbohydrates than Sea HA. HMA has the lowest nitrogen content, which indicates the lowest content of amino acid residues in that fraction. Glebova [18] has found that HMA contains more polysaccharides than amino acid residues. These subunits may cause better solubility of HMA in water as compared with HA.

Table 2. Elementary composition of HS in the sea and lake sediments

Humic substances	Ash, %	In organic matter, %				[H]/[C]	[O]/[C]	[N]/[C]
		C	H	N	O			
Sea HA	33.0	50.3	7.5	7.2	35.0	1.79	0.52	0.12
Ac.sea HA	48.8	47.7	7.4	6.8	38.1	1.86	0.60	0.12
Lake HA	7.8	43.5	6.8	4.0	45.7	1.88	0.79	0.08
Ac.lake HA	4.4	42.3	6.2	4.3	47.2	1.76	0.84	0.09
Sea HMA	11.8	54.0	6.8	2.9	36.3	1.51	0.50	0.05
Ac.sea HMA	12.1	54.5	7.2	3.1	35.2	1.59	0.48	0.05
Lake HMA	4.9	52.3	6.3	2.9	38.5	1.44	0.55	0.05
Ac.lake HMA	5.6	51.2	6.1	2.4	40.3	1.43	0.59	0.04
Sea.FA	16.6	43.8	5.8	7.7	42.7	1.59	0.73	0.15
Ac.sea FA	7.4	42.2	4.3	3.9	49.6	1.22	0.88	0.08
Lake FA	28.6	45.2	5.2	7.1	42.5	1.38	0.70	0.14
Ac.lake FA	39.0	42.0	4.1	4.4	49.5	1.17	0.88	0.09

The acid pre-treatment of the natural SM and LM diminished the content of carbon in most of the HS fractions. Goh and Reid [134] also described a similar effect. Nitrogen content in the Sea HA was ~1.6 times higher than that of Lake HA. After acid pre-treatment of the sediment, the nitrogen content in the Sea FA and Lake FA diminished by about two times. This means that amino acid residues, the main source of nitrogen in FA, are released from FA in the course of acid treatment.

To characterize elemental composition, atomic ratio of the elements is often used. It is known that the [H]/[C] ratio is connected with the ratio of aliphatic/aromatic compounds and indicates the amount of saturated C atoms and/or branched structures within a molecule [13,135]. In our case, the obtained ratio of more than 1.4 indicates that the aliphatic groups dominate over aromatics. The highest aliphatic nature was found for HA fractions. It is in good accordance with earlier findings [136].

FA has more unsaturated structures than HA. The acid pre-treatment increases the aromaticity in Lake HA, HMA, and Sea FA fractions. This conclusion is also supported by the UV-spectra of the fractions (Table 5).

[O]/[C] ratio is assumed to indicate the degree of oxidation of HS and also the carbohydrate presence [10,135]. We have found that FA has a higher oxygen content – consequently more oxygen containing groups. It is known that FA has more carbohydrates than HA [14,19]. The acid pre-treatment increased the content of these groups.

[N]/[C] ratio in HA and FA is high. The same result was obtained for HA from different sediments of lakes and rivers [16,136,137]. The high [N]/[C] ratio for the sedimentary HS, in comparison with soil and water HS, is supposed to be because of their precursor material constitutes mainly phytoplankton [16].

According to the data in Table 2, we may conclude that both Sea and Lake HA are more aliphatic than other HS fractions. Lake HA and FA from both sources have the highest carbohydrate content. HMA have the highest aromaticity and the lowest content of amino residues. Thus, extracted Sea and Lake HS fractions have quite ordinary elementary composition, although their origins are different.

5.1.3. Metals in the sediments and HS fractions

In order to establish the metal distribution in the course of separation (Article I) and to obtain information about affinity of the cations towards HS, we determined the content of Pb, Hg, Cr, Fe, Zn, Cu, Mg, and Mn in the sediments and its HS fractions. The results are presented in Tables 3 and 4.

Table 3. Concentration of metals (mg/kg dry weight of sediment) in the sea and lake sediment

Sediment	Fe	Zn	Cu	Mg	Mn
Sea sediment (SM)	2641	107	53	8616	28
Lake sediment (LM)	1520	60	71	3440	96

In the SM and LM as well as in their HS fractions, we found that the concentration of heavy metals Pb and Cr is lower than <0.08 mg/kg. The concentration of Hg in the LM was 0.30 mg/kg and 0.08 mg/kg in the SM. As expected, the metal concentration is considerably lower in the LM than in the SM, which is characteristic of the sediment of this kind because of the conditions of their genesis.

As can be seen from Table 4, the concentration of metals varies in HS fractions.

Sea sediment. We observed that Fe, Mn and Mg are concentrated into the HA. The acid pre-treatment increased the concentration of Fe, but the concentration of Mn and Mg did not change. Cu and Zn were concentrated into the HMA, but the acid pre-treatment increased the concentration of Zn and decreased the concentration of Cu in HMA. Cu was also concentrated in FA. However, the acid pre-treatment reduced its amount considerably (Cu is extracted into acid). Mn was found neither in HMA nor in FA. The result is in

good accordance with the literature, claiming that HA from different sources contains more Mn complexes than other HS fractions [113].

Lake sediment. We have found that Mg is concentrated into HA and HMA. The acid pre-treatment increased the concentration of Mg in HA and decreased it in HMA. Cu was not found in HA. Cu and Zn were also concentrated into the HMA. The acid pre-treatment decreased the concentration of Zn and Cu in this fraction. The concentration of Zn in FA was also considerable. The acid pre-treatment increased the concentration of Zn in FA. Mn was found neither in HMA nor in FA.

If we suggest that the differences in the metal cation distribution are due to their ability to form complexes with HS, we may assume that the five metals investigated are concentrated differently in the SM and LM HS fractions. Those differences should be related to HS natural structure. Thus, HA should have more of those functional groups that prefer to bind with Fe and Mn. In HMA structure, there should be more Zn and Cu binding sites. Initial Mg prevails to form complexes with Sea HA and Lake HMA.

Table 4. Concentration of metals in different HS fractions in the sea and lake sediment

		TMC ^a			HA ^b		HMA ^b		FA ^b	
		mg/kg	mg/kg	%	Mg/kg	%	mg/kg	%	mg/kg	%
Zn	SM	1264	270	21.4	933	73.8	61	4.8		
	Ac.SM	1742	310	17.8	1380	79.2	52	3.0		
	LM	253	55	21.8	144	56.9	54	21.3		
	Ac.LM	118	40	33.9	19	16.1	59	50.0		
Cu	SM	1484	250	16.8	897	60.5	337	22.7		
	Ac.SM	705	250	35.5	420	59.5	35	5.0		
	LM	215	nd		183	85.1	32	14.9		
	Ac.LM	68	nd		19	27.9	49	72.1		
Mn	SM	40	40	100	nd		nd			
	Ac.SM	40	40	100	nd		nd			
	LM	18	18	100	nd		nd			
	Ac.LM	nd	nd		nd		nd			
Mg	SM	1166	710	60.9	395	33.9	61	5.2		
	Ac.SM	1046	710	67.9	240	22.9	96	9.2		
	LM	387	146	37.7	209	54.0	32	8.3		
	Ac.LM	326	170	52.1	97	29.8	59	18.1		
Fe	SM	1134	1090	96.1	24	2.1	20	1.8		
	Ac.SM	1747	1680	96.1	50	2.9	17	1.0		
	LM	112	64	57.2	26	23.2	22	19.6		
	Ac.LM	98	20	20.4	58	59.2	20	20.4		

^a – total metal concentration (mg/kg dry weight of HS fraction) in sum of the HS fractions of selected sediment.

^b – metal concentration of the HS fraction in mg/kg and % from TMC.

nd – not detected at the detection level.

Comparing the data from Tables 1, 3, and 4, we can see that HS fractions bind very small quantities of metals from natural sediments. Sea HS, as a sum

of HA, HMA and FA, binds more Cu (3.6% of total Cu from the SM) and Zn (1.2% of total Zn). Most of Fe and Mg remain in the sediment. HS contain only 0.07% of Fe and 0.02% of Mg from total Fe and Mg concentration in SM. Lake HS bind more Zn, about 3.6% of total Zn and Cu, about 1.0% of total Cu from the LM. Lake HS fractions are complexate with 0.14% of Mg and 0.13% of Fe from total Mg and Fe concentration in the LM. Differences between complexing Zn and Cu in Sea and Lake HS are related to the differences in their structure.

To compare the amount of metals in HS before and after dividing in fractions, metal concentration of the alkaline HS extract of the SM is presented in Figure 1. Alkaline treatment removed 7.9% Cu, 5.2% Zn, 3.8% Fe and 0.8% Mg, from the SM. We found that, in the HA, HMA and FA (as a sum), there was only 1.7% of Fe, 2.1% of Mg, 23.2% of Zn and 45.2% of Cu left from the total amount of those metals after the alkaline HS extraction. This means that Cu is the metal most strongly bound to HS. The result is in good accordance with the literature data, showing the order for the stability of the metal/HS complexes to be Cu>Zn>Mg>Fe [89].

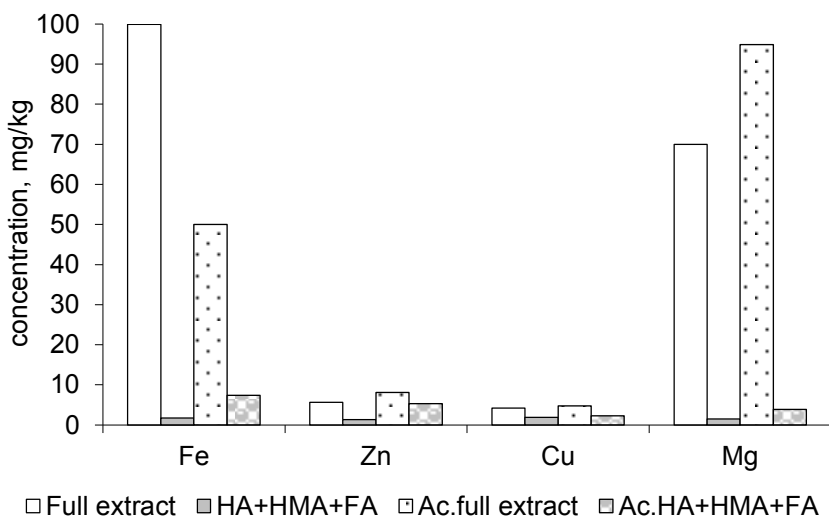


Figure 1. Concentrations of metals in mg/kg dry weight of sediment in the alkaline HS extract of natural and acid pre-treated sea sediment and in sum of the HS fractions (HA+HMA+FA)

The acid pre-treatment of SM decreased the total metal content of Cu, Mg, Zn, and Fe in the alkaline HS extract 0.9 times as compared with that of natural alkaline HS extract. We found that the acidification of sediment increased the Mg content in 35%, Zn content in 45% and Cu content in 14% in the HS fractions. At the same time, the content of Fe decreased 50%. After acid pre-treatment there was only 4.1% of Mg, 14.8% of Fe, 47.9% of Cu, and 65.4% of Zn extracted from the total amount in SM. We may suppose from the different metal content in the HS fractions that the acidification of natural SM changes the structure of HS fractions (Table 4). These findings support the idea that the

complexation properties of HS fractions may give us information about the structure of the fraction.

5.1.4. UV-VIS spectroscopy and calculated aromaticity

All humic samples exhibit a featureless increase in absorbance with a decreasing wavelength. The ultraviolet spectra of HA, HMA and FA are similar, differing only slightly in optical density. We measured molar absorptivities of our HS fractions at 280 nm. The procedure is described in Article I. This wavelength was chosen because π - π^* electron transitions occur in this region of the UV range for phenolic substances, aniline derivatives, benzoic acids, polyenes, and polycyclic aromatic hydrocarbons. Many of these compounds are considered common structural subunits in the humic matter [138,139]. Since many of these substances are precursor components of certain types of HS, molar absorptivity ϵ may serve as a basis for calculation of aromaticity of humic matter and for evaluation of its origin. The following equation was used [139,140]:

$$\text{Aromaticity} = 0.05 \epsilon + 6.74, \quad (1)$$

where ϵ is molar absorption, $l (\text{molC})^{-1} \text{cm}^{-1}$

Table 2 shows that HS fractions contain inorganic salts (ash). Therefore, the molar absorptivity ϵ is calculated on a mole of organic carbon, instead of the weight of humic matter per unit volume water [138,139]. Spectroscopic properties and the value of calculated aromaticity of HS fractions are presented in Table 5.

Table 5. Spectroscopic properties of HS fractions

HS fraction	E2/E3	ϵ	Aromaticity, %
Sea HA	3.49	130	13
Ac.sea HA	3.42	298	22
Lake HA	3.14	88	11
Ac.lake HA	2.82	188	16
Sea HMA	3.91	558	35
Ac.sea HMA	3.50	536	34
Lake HMA	3.82	506	32
Ac.lake HMA	3.55	674	40
Sea FA	4.48	262	20
Ac.sea FA	4.55	333	23
Lake FA	4.04	227	18
Ac.lake FA	4.94	197	17

Peuravuori and Pihlaja [138] have found that the correlation between the quotient E2/E3 (ratio of absorbances at 250 and 365 nm) and molar absorptivity at 280 nm is quite moderate for the isolated HS fractions. In our fractions, this

correlation is moderate too. Therefore, a comparison of molar absorptivities and calculated values of aromaticity (Table 5) allows us to evaluate how HS structure and properties depend on their origin. No sources available to us provide data about the spectroscopic properties of HMA. We established that HMA had the highest molar absorption and calculated aromaticity.

We looked for a possible correlation between calculated aromaticity in Table 5 and the concentration of Mg, Fe, Zn and Cu in different HS fractions in Table 4. However, for Mg and Fe, we did not find any correlation between the concentration of the metal with the aromaticity. Thus, the complexation of those metals is not related only to the aromatic functional groups. The calculated aromaticity value correlated quite well with the amount of Cu and Zn (Figure 2) in the fractions (in Sea HS $R^2_{Cu} = 0.9634$, $R^2_{Zn} = 0.7284$ and in Lake HS $R^2_{Cu} = 0.9717$, $R^2_{Zn} = 0.8868$, correspondingly). It may be supposed that aromatic structures (such as acids and phenols) are the important chelating substances for those metals. Fe prevails HS fractions with low aromaticity, i.e. HA fraction in SM and in LM.

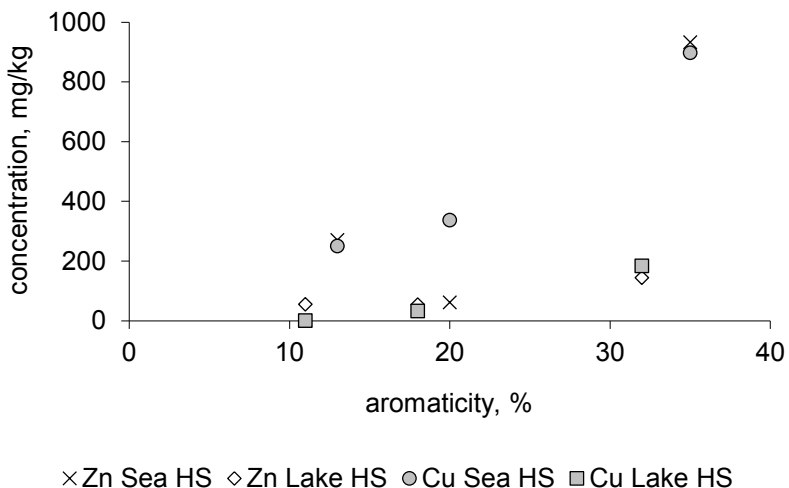


Figure 2. Correlation of concentration of metals (Zn, Cu) in mg/kg in different natural sea and lake HS fractions with calculated aromaticity of those HS

We found that aromaticity in HS fractions grows in the following order: HA<FA<HMA. Sea HS fractions have higher aromaticity and contain more Zn and Cu. Comparing the elemental composition from Table 2 with the calculated aromaticity, we observed that C content in the organic matter of the humic fraction increases and O content decreases. It is suggested that HMA always contains aromatic and quinodal cores, bound together through C-C or C-O-C bridges, phenolic hydroxyl, carboxyl groups, and short aliphatic chains [17]. HMA having the highest aromaticity contains many phenolic hydroxyl and carboxyl groups that may bind Cu and Zn. At the same time, HA has a more

aliphatic structure, not capable of binding metal, which explains the low content of those metals in this fraction.

5.2. The precipitation ability of Zn^{2+} , Mg^{2+} , Mn^{2+} , Pb^{2+} , Cu^{2+} with different HS fractions (Article II)

When metal cations bind to the HS structure, the negative charge of the cluster is reduced, leading consequently, to a reduction in intermolecular repulsion between HS subunits. At neutral pH, HS carry significant negative charges in solution due to dissociated carboxylic groups. In order to achieve flocculation it is necessary to reduce that negative charge significantly. Metal binding influences the charge neutralization and induces the aggregation of metal/HS complexes. Further addition of metal produces progressively higher and higher degrees of aggregation, as the charge of HS is further reduced and the repulsion tends towards zero. Eventually, the charge is reduced to a sufficient level and the precipitation of HS from solution begins. The multicharged metal ions may influence the HS structure, when they form covalent bonds with neighbouring functional groups. These considerations are consistent with the observation that hydrophobic zones are formed when metals are added to HS [86]. In the absence of metal ions, the dissociated functional groups produce a hydrophilic hydrated structure. When the charge is neutralized, the HS wrap around the metal ion, resulting in a hydrophobic region and presumably, the exclusion of the water. It is possible that the metals have a double effect: they promote aggregation by reducing electrostatic repulsion, and enhance further the tendency for flocculation, producing more hydrophobic structures, thus increasing the attractive forces between HS molecules. Ions of higher charge would be more effective at charge neutralization, inducing structural rearrangements and the formation of hydrophobic zones. Although metals bind rapidly to HS, there is some subsequent structure rearrangement, resulting in stronger binding. Because of that, more time is required for flocculation. It is possible that the metals also promote aggregation by the formation of hydrophobic zones around their binding sites in the otherwise hydrophilic, solvent-penetrated HS structure [86].

In this work, the specific precipitation of metals with different HS fractions was studied. It is the first attempt to characterize and compare HMA interactions with metals and with other HS fractions. The precipitation procedure and the results obtained are described in Article II.

5.2.1. Effect of pH on the precipitation ability of Zn^{2+} /Sea HS complexes

It is known that the ability of HS fractions to bind metals depends strongly on the pH of the medium. The maximum metal sorption capacity is achieved at neutral or at slightly acidic pH [89]. We used Zn^{2+} as a model cation. In order to follow the pH dependence of precipitation, we investigated the behaviour of Zn^{2+} /Sea HS complexes at different pH values (pH 4-8; Figure 3).

From the SM HS fractions, HA revealed the best precipitation ability in the whole investigated pH range. However, only at higher pH values HA exhibited better precipitation. At pH 4 HA precipitated more Zn^{2+} than HMA and FA. HA and FA revealed a steady increase in precipitation from pH 4 to pH 8, while HMA gave a maximum (at pH 7). FA had the lowest precipitation ability at pH 5 to pH 7 – consequently, Zn^{2+} /FA complexes are more soluble than other HS complexes, only slightly depending on the pH value. HMA possessed the lowest precipitation ability at lower pH values (up to pH 5), but already at pH 7, precipitation considerably increased. Therefore, for the following experiments we used pH 7, which is suitable for all HS fractions.

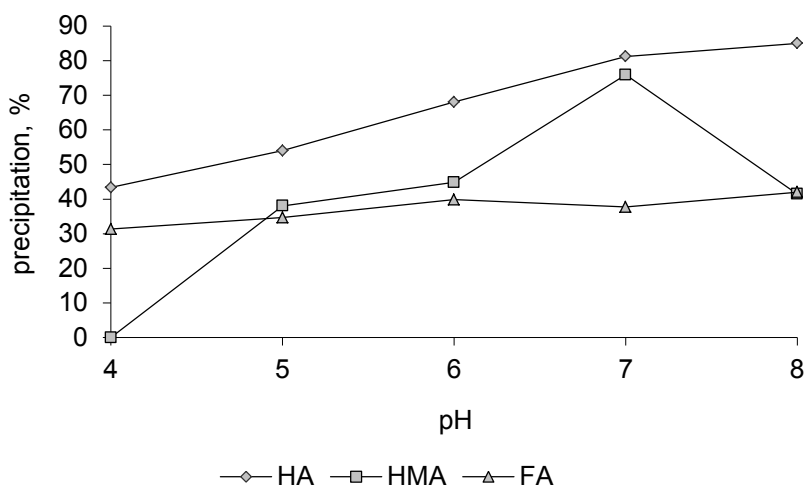


Figure 3. Precipitation (%) of different Zn^{2+} /Sea HS complexes in different pH values (Concentration of HMA 0.1 mg/ml; FA 1.25 mg/ml; HA 2.5 mg/ml; Zn^{2+} concentration 0.4 mmol/g)

5.2.2. Precipitation of Zn^{2+} by HS fractions at pH 7

It is known that migration abilities of HS depend on the metallic ion, the cation charge, the degree of ionization of the organic molecule, the ionic strength of the media, and the location of the metal ion. Also, the precipitation of HS depends on the same factors [85]. We have already mentioned the general types of functional groups in HS: -COOH, enolic-, aliphatic-, phenolic-OH, C=O; nitrogen and sulphur containing groups. It is obvious that their content influences the formation of different metal complexes.

Concentration of the obtained water-soluble HS fractions in SM and LM is very low. To reach a result closest to the real environment, the obtained fractions were not lyophilized or dried. However, the Zn^{2+} concentration was calculated on 1 g of the weight of the corresponding dry HS fraction. The precipitation of Zn^{2+} in different HS fractions is presented in Figure 4.

The concentration of the investigated HA and HMA varied from 0.1 mg/ml to 2.5 mg/ml. The concentration of different FA varied from 0.16 mg/ml to 1.25 mg/ml. In the case of HA and HMA (from both sediment), the amount of precipitated Zn^{2+} exhibited a linear correlation from the amount of added Zn^{2+} ($R^2 = 0.9846 - 0.9995$). FA had the correlation of a slightly different shape, however, it may be still handled, according to the linear correlation equation (for Sea FA, $R^2 = 0.9769$ and for Lake FA, $R^2 = 0.9221$) and that indicates clearly to the dependence from the ion concentration. The slope of the line is different for each HS fraction in SM and LM: for HA ($R^2_{Sea} = 0.7165$ and $R^2_{Lake} = 0.7719$); for HMA ($R^2_{Sea} = 0.6711$ and $R^2_{Lake} = 0.6793$); for FA ($R^2_{Sea} = 0.4405$ and $R^2_{Lake} = 0.5190$). Those data showed the precipitation order of Zn^{2+} /HS complexes: HA>HMA>FA.

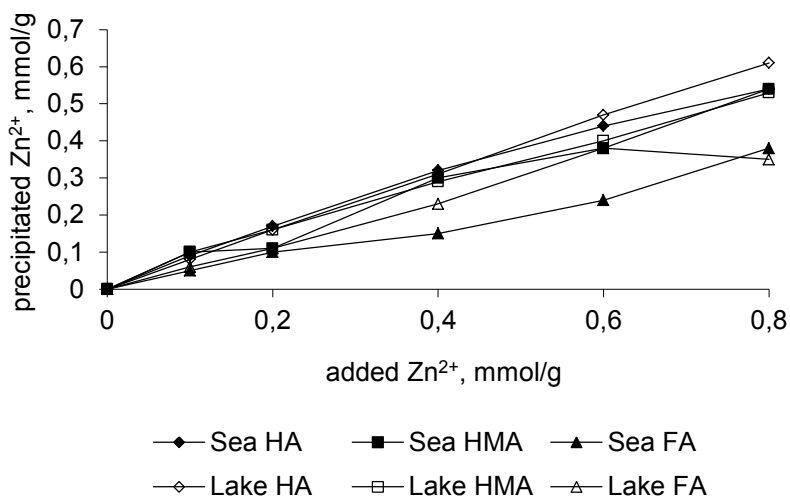


Figure 4. Precipitation ability of Zn^{2+} (mmol/g of HS) at pH 7 (Concentrations of HS fractions: Sea HMA – 0.1 mg/ml, Lake HMA – 0.12 mg/ml, Lake FA – 0.16 mg/ml, Sea HA – 2.5 mg/ml, Lake HA and Sea HA – 1.25 mg/ml)

The Lake HA revealed the highest precipitation ability (from the 0.8 mmol/g of added Zn^{2+} 0.61 mmol/g was precipitated). We did not measure the maximum capacity of the Zn^{2+} precipitation by HS. However, according to our data it is certainly higher than the value obtained for coal derived HA [89]. According to their analysis, the solid HA from coals bound 0.43 mmol/g of Zn^{2+} . The result obtained by us may be connected with the use of non-dehydrated samples (to avoid the structure changes) and with the structure of HA from various sources. Martyniuk and Więckowska [81] have also found that HA gels bind more metals than HA solutions that are made from the lyophilized product. If the ratio of Zn^{2+} and HS is kept constant, there are no significant differences in the precipitation ability of both Sea and Lake HMA and HA at different concentrations (0.1 to 2.5 mg/ml). The ratio of precipitated and added Zn^{2+} is almost linear. Small differences were observed in the case of FA because their Zn^{2+} complexes have better solubility at pH 7. The Zn^{2+} /Sea FA

complexes are more soluble at a constant metal/FA ratio than Zn^{2+} /Lake FA complexes. It may be related to the higher content of carbohydrates in the Sea FA than in the Lake FA [14]. According to those results, it is possible to use different HS to investigate their precipitation.

From those data of precipitation experiments we can distinguish two groups of HS: 1) HA and HMA; 2) FA. This difference in precipitation was observed also at lower Zn^{2+} concentrations: good precipitation ability was observed for both HA fractions (83–88% of the Zn^{2+} amount was precipitated). However, the highest precipitation ability was observed for both HMA fractions, resulting in complete precipitation of the added metal. The slight decrease in the precipitation ability of the Sea HA at higher Zn^{2+} concentrations may be caused by the high initial concentration of Zn^{2+} in that fraction (the initial Sea HA had five times more Zn^{2+} than the Lake HA, Table 3). Approximately 68% of the Zn^{2+} amount was precipitated with the Sea HA at the highest metal concentration. The Lake FA precipitated slightly more Zn^{2+} than the Sea FA.

5.2.3. The precipitation ability of HA by different metals

In order to compare directly the precipitation ability of HA from different sources (SM or LM), metal cations in separate solutions (0.6 mmol/g of each metal: Pb^{2+} , Cu^{2+} , Mn^{2+} , Mg^{2+} , Zn^{2+} , at pH 7) were added to HA. The amount of equilibrium concentrations of metals that remained in the solution after co-precipitation of the metal with HA was measured (calculated on the amount of the precipitated metal). The results obtained are shown in Figure 5.

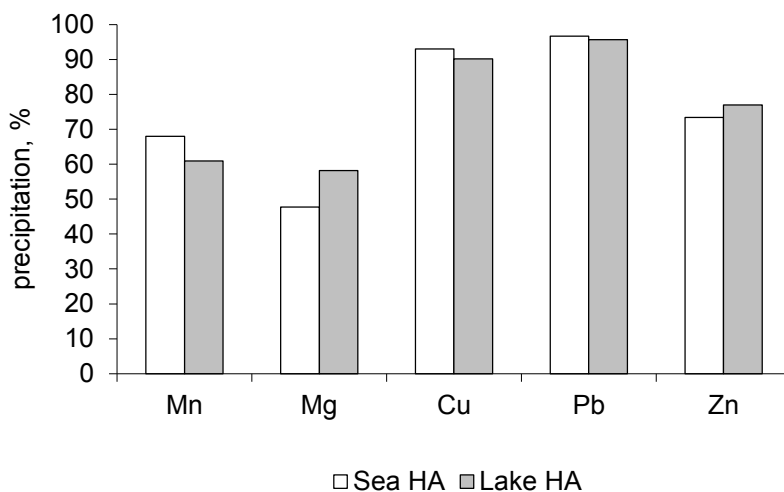


Figure 5. Precipitation of different metal/HA complexes at pH 7 (HA concentration is 2.5 mg/ml and metal concentration 0.6 mmol/g)

The metals are able to form chemical bonds with the functional groups of HS, neutralizing the electrical charge of the natural HS. When the charge is

sufficiently reduced, HS precipitate from solution [86]. Therefore, addition of metals could cause instability of the initial metal/HA complexes and gives rise to aggregation. Previous results have suggested that higher atomic weight metals give better chemical affinity to HA [81]. We have found that the heavy metals Pb^{2+} and Cu^{2+} precipitate better with both Sea and Lake HA. In addition, both Lake and Sea HA fractions gave the same metal cation precipitation order: $Pb^{2+} > Cu^{2+} > Zn^{2+} > Mn^{2+} > Mg^{2+}$. Similar stability orders of metal/HA complexes are reported in the literature: $Cu^{2+} > Pb^{2+} > Zn^{2+} > Mn^{2+} > Mg^{2+}$ for soil HA [92]; $Cu^{2+} > Pb^{2+} > Zn^{2+}$ for river sediment HA [16] and $Pb^{2+} > Cu^{2+} > Zn^{2+} \sim Mn^{2+} > Mg^{2+}$ for coal HA [89]. The differences in the Sea and Lake HA are also not considerable, however, the former precipitates slightly better with Pb^{2+} , Cu^{2+} and Mn^{2+} , but the latter with Zn^{2+} and Mg^{2+} .

5.2.4. Stability constants of precipitated metal/HS complexes

As reported by Pandey et al. [92], the stability constants of the metal /HS complexes are conditional and are valid only for the conditions under which they were determined. In our case, the calculated conditional stability constants are valid for metal/HS complexes after three days of the addition of the metal. The equation describing the formation of the precipitating complex is as follows:



where M is Mn^{2+} , Mg^{2+} , Cu^{2+} , Pb^{2+} or Zn^{2+} , HS is the specific fraction of HS.

Calculations were made with the use of the following equation [109]:

$$K = C_{M \text{ bound}} / (C_M C_{HS}), \quad (3)$$

where K is the stability constant of the metal complex with the respective fraction of HS, $C_{M \text{ bound}}$ is the concentration of the metal that retained in the precipitate, C_M is the concentration of metal in solution, C_{HS} is the concentration of HS fraction recalculated for organic carbon. $C_{M \text{ bound}}$ was calculated as follows:

$$C_{M \text{ bound}} = C_{Mi} + C_{MN} - C_M, \quad (4)$$

where C_{Mi} is the concentration of the inserted metal and C_{MN} is the initial concentration of the metal in the related HS fraction.

In the calculated stability constant, the metal concentration was 0.6 mmol/g of each metal in the separate HS solution. The results are given in Table 6.

The highest values were obtained for Pb^{2+} and Cu^{2+} complexes. We compared the Zn^{2+} complexation with different fractions and found the highest calculated stability constant for Zn^{2+}/HMA and $Zn^{2+}/Lake \text{ FA}$ complexes. This is in good agreement with the calculated aromaticity values for HS fractions

(Table 5). Therefore, HMA fractions had the highest aromaticity and the calculated stability constant. It may be supposed that aromatic acids and phenols are the most important binding sites for the Zn^{2+} cation.

Table 6. Calculated stability constants of different metal/HS complexes (The metal concentration is 0.6 mmol/g of HS and pH 7)

Metal	HS	Concentration of HS (mol/l)	$C_{M\ bound} / C_M$	Log K
Zn^{2+}	Sea HA	0.07	2.97	1.63
	Sea HMA	0.004	1.85	2.67
	Sea FA	0.04	0.69	1.24
	Lake HA	0.04	3.55	1.95
	Lake HMA	0.005	1.96	2.59
	Lake FA	0.004	1.70	2.63
Mn^{2+}	Sea HA	0.07	2.13	1.48
	Lake HA	0.08	1.56	1.29
Mg^{2+}	Sea HA	0.07	0.91	1.11
	Lake HA	0.08	1.39	1.24
Cu^{2+}	Sea HA	0.07	13.3	2.28
	Lake HA	0.08	9.14	2.06
Pb^{2+}	Sea HA	0.07	29.2	2.62
	Lake HA	0.08	22.0	2.44

5.3. Capillary electrophoresis and HS (Article III)

During recent years, CE has been used for the characterization of HS and in the area of metal analysis [5,8,22,24,55,56,77,101,116-122]. The typical wavelength for the determination of HS in CE is 254 nm. However, in many occasions, different other wavelengths are used in CE, depending on the UV-detector and on the buffer. For example, for the characterization of HS 230 nm [66], 220 nm [55] have been used. In many other cases, various UV wavelengths have been used: metal cations, inorganic anions, and organic acids – 225 and 230 nm [141,142]; pesticides – 226 nm [143]. We used lower wavelength (226 nm) to achieve somewhat stronger absorption intensities than those did at 254 nm [59].

Lee and Lin [144] have found that the best for separation of metal cations by CE is achieved with UV-absorbed component (imidazole) and complexing agent (different carboxylic acids). Typically, for CE of HS different BGEs are used and HS are injected as a sample to the BGE solution. From the obtained electropherograms many authors omitted reference to the fact that a number of peaks could be a system peaks, which are only due to the used buffer from BGE. Due to the anionic character of HS, it becomes clear that any type of cationic buffer will be able to interact in some extent with some fractions of HS [4,22,67]. Schmitt-Kopplin et al. [56] found that FA always showed higher polydispersities than HA. Several separated sharp peaks in electropherograms

corresponding to lower-molecular-mass compounds, which were found in the FA, but never in the HA. These phenolic acids could have been released in solution by partial hydrolysis of the FA. Pokorna et al. [8] found some small peaks in coal derived HA electropherograms that cannot be identified.

We suggested that HS (in the structure are many carboxylic groups) could also act as complexing agents together with imidazole in separating metal cations. Also, we wondered whether HS fractions/imidazole could be used as BGE in the CE analysis. However, the interpretation of the recorded electropherograms failed because many randomly distributed spikes appeared. The frequency of the appearance of spikes depended on the applied voltage and on the concentration of the HA in the buffer. Also, a clear dependence on the sample preparation conditions and buffer composition was evident. For that reason, the properties of HS and imidazole-HA as BGE in electric field were investigated.

5.3.1. Flow of HA solution in capillary without applying electric field

In this study, we used HS as a BGE in capillary electrophoresis. The procedure and the results are presented in Article III. First, for the characterization of the behaviour of HA in capillary we passed the samples of HA without applying voltage (see Table 1 in Article III). Thus, we pumped samples through the capillary at a constant flow rate. We observed the appearance of several spikes in the UV detector signal from some of the working solutions (see Figure 1 in Article III).

The filtration of the working solutions (solutions C, D and F) reduced the number and intensity of the spikes. The dependence of results on HA concentration indicate trivially that the appearance of spikes from unfiltered solutions can be associated with the presence of possible aggregate particles in the HA solution, which either absorb or scatter UV light from the detector. When imidazole is added to BGE, a significant reduction of the amount of spikes on the filtered solutions (C and F) signal is observed, possibly because of a considerable increase in the solubility of HA in water and the reduction of size of the formed aggregates.

5.3.2. Pumping HA solution with applying electric field

When pumping the solution A through the capillary and applying the high voltage (30 kV) to the capillary, the frequency of the observed spikes increased to some extent, starting from the moment when voltage was applied (see Figure 2, solution A, in Article III). However, this increase can be fully associated with the effect of the increased flow velocity of the solution because the EOF speed adds to the pumping flow.

We measured the mean number of spikes over a time span from 0 to 10 min (pump only on, voltage not applied) and from 15 to 25 min (pump and voltage both applied) with 1 min increment (10 determinations over the interval $\Delta t = 1$

min). We obtained the following results: spikes when pumping only $n_{pump} = 15.3 \pm 2.2$; and spikes when pumping at high voltage $n_{EOF+pump} = 25.2 \pm 6.8$ (n_{pump} and $n_{EOF+pump}$ are the mean numbers of spikes with voltage off (from 0 to 10 min) and voltage on (from 10 to 25 min, respectively). The corresponding flow rates were calculated as follows:

$$F_{pump} = v_{pump} \pi d^2 / 4 \quad (5)$$

$$F_{total} = (v_{pump} + v_{EOF}) \pi d^2 / 4 \quad (6)$$

The flow rate for 30 kV was $F_{pump} = 2.83 \cdot 10^{-7} \text{ ml s}^{-1}$ and $F_{total} = 5.03 \cdot 10^{-7} \text{ ml s}^{-1}$.

The velocity of the EOF increases linearly with the applied voltage, however, the apparent frequency of spikes increases even if the concentration of possible absorbing species remains unchanged. To obtain a quantitative measure of absorbing species concentration as a function of applied voltage and correct results for the EOF influence, the number of spikes n , the height of which exceeded the preset threshold, was counted after a fixed time interval Δt . The threshold value was three times the baseline noise standard deviation. This number was averaged against the overall measurement time.

Then, the aggregate concentration can be estimated as follows:

$$c_{aggr} = \frac{n}{(F_{EOF} + F_{pump}) \Delta t}, \quad (7)$$

where F_{EOF} and F_{pump} are EOF and pump flow velocities.

Electrophoretic mobility was calculated according to Schmitt-Kopplin et al. [56]. From the results of EOF flow rate measurements, the calculated EOF mobility was equal to $(1.44 \pm 0.02) \cdot 10^{-3} \text{ cm}^2 \text{V}^{-1} \text{s}^{-1}$.

By the use of Eq. (7), aggregate concentration is $c_{pump} = 9.0 \cdot 10^5 \text{ ml}^{-1}$ without applied voltage and $c_{pump+EOF} = 8.4 \cdot 10^5 \text{ ml}^{-1}$ with applied voltage.

Considering relative standard deviations of flow rate and time measurements negligible, as compared to the relative standard deviation of a spike number, the standard deviation for aggregate concentration during the flow without applied voltage s_c^{pump} , estimated by Eq. (7) was:

$$s_c^{pump} = c_{pump} (s_n^{pump} / n_{pump}), \quad (8)$$

where s_n^{pump} is a standard deviation of the number of spikes. The standard deviation from Eq. (8) was $1.3 \cdot 10^5 \text{ ml}^{-1}$. A similar calculation gives $s_c^{pump+EOF} = 2.3 \cdot 10^5 \text{ ml}^{-1}$.

Filtration of the solution A (resulting in solution D) removed almost all spikes in electropherograms (see Figure 2, solution D, in Article III).

In the case of solution B (HA in the presence of imidazole), when applying the electric field, a profound effect of aggregation was observed. The increase of the frequency of the spikes (see Figure 2, solution B, in Article III) is evident and can be associated with an increase in aggregate concentration without any statistical scrutiny. A similar phenomenon was observed for colloidal particles in the electric field, where even clear hysteresis cycle was obtained when high voltage at different values was applied [145]. The figures reveal that the aggregation is enhanced by the presence of imidazole. This result may be connected with the formation of imidazolium complexes with HA molecules. Blank imidazole solution (10 mM of imidazole) did not exhibit any spikes on the electropherogram, being just a baseline without any features. The following HA measurements were performed only with working solutions containing imidazole.

Effect of concentration and filtration of HA solution. The used buffer is similar with those used by Lee and Lin [144] for the determination of metal cations. As expected, the frequency of spikes was higher in a more concentrated solution (see Figure 3, in Article III). Also, the frequency of spikes was lower in the filtrated solution (see Figure 4, in Article III). Those Figures show that the appearance of spikes is strongly influenced by the applied voltage. This fact might well explain the nature of spikes encountered in many published electropherograms of HA capillary electrophoresis (see, e.g. [57]). At high HA concentrations ($> 0.2 \text{ mg ml}^{-1}$ used e.g. in [22]), spikes on “hump” might have appeared because of the aggregation of the sample subjected to high voltage during the CE run. The filtration did not remove particles that form and aggregate at high voltage.

Effect of the electric field. Although the aggregation is influenced by the concentration of HA, the value of the applied voltage has a profound effect on aggregate formation, as it was stated already above. By pumping the solution E through the capillary at a constant rate and applying voltages from 5 to 30 kV, the frequency of spikes increased considerably (Figure 6).

From that result, the concentration of aggregates as a function of the applied voltage was calculated according to Eq. (7). The results revealed that the increase in the voltage clearly supports aggregation (Figure 6). It is still not clear what type of mechanism is responsible for this behaviour. The reason for aggregation may be either a distribution of the size to the charge ratio of the aggregates or changing the double layer of the aggregate surface under the applied electric field, thus reducing the electrical repulsion of aggregates. In addition, as speculated by Zheng and Yeung [69], particles may have different shapes and orientation in relation to the electric field in the capillary. All of those facts could result in a different mobility of different aggregate particles and this, in turn, could result in their collision and cluster to the larger aggregates.

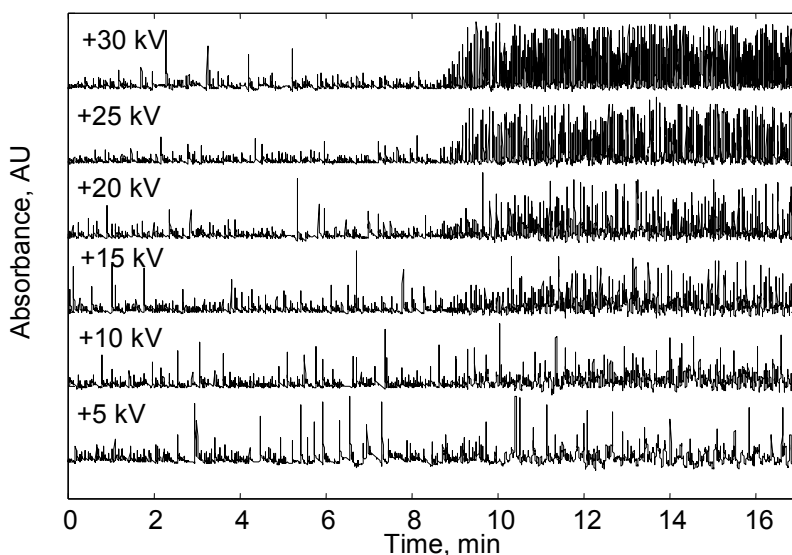


Figure 6. UV absorbance signals of solution E using pump at constant rate, different voltages applied at 9 min, UV at 226 nm

The results obtained are in good accordance with the suggestion made earlier by different authors: the aggregates are formed during a CE run and each aggregate can randomly be retarded in the capillary [146,147], and do not support Pokorna et al. [57] who suggested that the spikes in electropherograms correspond to the different compounds present in HA that are liberated from the supramolecular structure of the HA.

5.3.3. Comparison of the behaviour of cyclodextrin (CD) and HS solutions in the electric field

HA solution has colloidal properties at higher pH ($\text{pH} < 9$). At the same conditions, other HS fractions (HMA and FA) that have no colloidal properties did not show the spikes (electropherograms reveal only baseline).

We suggested that the aggregation phenomenon is not connected only with HA but is a more general phenomenon associated with any of organic molecules that form colloidal particles. Indeed, recently it was observed that such an aggregation takes place in the high voltage electric field [145]. In order to prove that suggestion we investigated the behaviour of more definite colloidal solutions in high voltage electric field. It is generally known that oligosaccharides are typical molecules that form colloidal systems at higher concentration and are charged only at very high pH [61]. When pumping β -CD solution (0.2 mM and 15 mM) through the capillary at 30 kV voltage no spikes were observed at lower concentration. However, at higher concentration, like it is the case with HA, similar spikes appeared when high voltage was applied (see Figure 7, in Article III). Indeed, in the case of CD solution it is unlikely that

imidazole may cause the appearance of charged particles (e.g. salt formation) and therefore, aggregation. Thus, these results show that the appearance of spikes is a general property of colloidal solutions, due to the aggregation of different organic molecules. That phenomenon is not necessarily associated with the properties of HS. In the case of HS, aggregation process will depend strongly upon the structure and nature of HS fraction [86].

5.4. Interactions of Pb^{2+} and Zn^{2+} with HS by electrophoretically mediated on-capillary microanalysis

When metal ions are added to the capillary with HS as BGE, metal ions mix with the HS, interact with them, and may form metal/HS complexes. The migration of the anionic HS and metal/HS complexes from the anode to the cathode is a net result of the electroosmotic and electrophoretic movement. This implies that the electrophoretic mobility of the negatively charged HS species is smaller than that of the EOF of the solution. The presence of metal ions changes the net charge of the HS and consequently, its electrophoretic properties [77]. Metal/HS complexes are generally negatively charged and moved toward the anode. The main anionic group of HS is carboxyl group. It is known that heavy metals complex better with HS [76,88,93] and Zn^{2+} forms weak complexes [16]. The mobility of all metals is reduced in the presence of HS. However, the mobility of Zn^{2+} is reduced less than that of Pb^{2+} . There can be two reasons for this: 1) the association of HS with Zn^{2+} is weaker than its association with Pb^{2+} , leaving relatively more free Zn^{2+} in solution; 2) the metal/HS complexes formed with Zn^{2+} were smaller and hence more mobile. Zn^{2+} /HS electrostatic interactions are important only at high local concentrations of the metal and do not produce complexes that are as strong and persistent as those formed with Pb^{2+} . The addition of metal ions to the HS solution undoubtedly leads to changes in aggregation [26].

Metal complexation is related to the different functional groups. Major binding sites are carboxyl and hydroxyl functional groups. The minor strong binding sites are nitrogen and sulphur bearing functional groups, which consist of a very large number of site types and so not forming a specific type of complexes [90]. It is known that Pb^{2+} complexed with HS *via* two different kinds on binding site: carbonyl and hydroxyl groups, and nitrogen containing moieties [16,90]. Zn^{2+} interacts with carboxyl, hydroxyl, thiol and amino groups [74]. In aquatic HS, Zn^{2+} complex better with carboxyl group [104,105], and in soil HS with thiol [105] and amino [91] groups. Zn^{2+} is relatively weakly complexed with HA [91].

In this thesis, the EMMA approach is used to explore complexation of Zn^{2+} and Pb^{2+} with different HS fractions from SM. The procedure is described in Article IV.

5.4.1. Interaction of Pb^{2+} with HS fractions (Article IV)

5.4.1.1. Electropherograms of HS fractions

When HS fractions are used as the BGE without adding metal salt, a steady baseline is obtained. After adding Pb^{2+} to the HS solution in CE, three main characteristic regions have evolved in the electropherogram. We investigated the behaviour of the all water-soluble HS fractions (HA, HMA and FA) used as a BGE together with Pb^{2+} solution. In all cases, we observed the formation of similar reproducible electropherograms but characteristic to each HS fraction. The typical electropherograms recorded after injection of $6 \cdot 10^{-4} \text{M}$ $\text{Pb}(\text{NO}_3)_2$ solution to the different BGE solutions are presented in Figure 7.

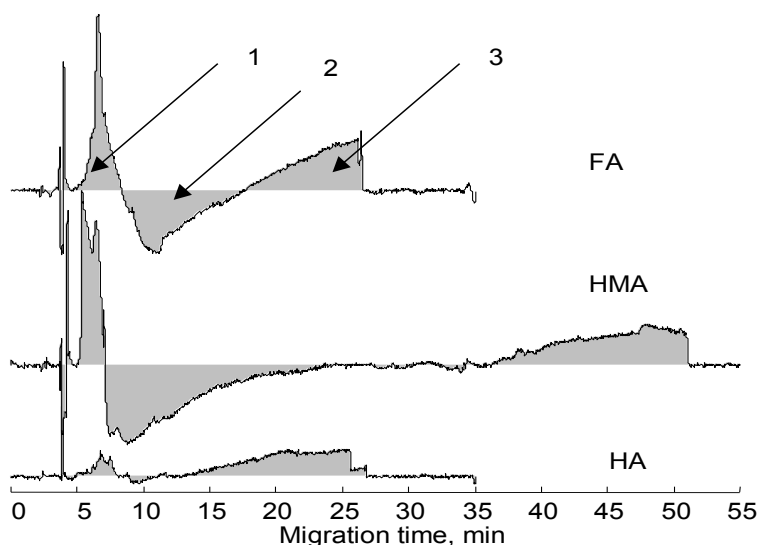


Figure 7. Electropherograms of Pb^{2+} solution when HA, HMA and FA were used as BGE (Separation voltage, 20 kV; hydrodynamic injection of $6 \cdot 10^{-4} \text{M}$ $\text{Pb}(\text{NO}_3)_2$, 15 s; pH 7; detection at 226 nm; fused-silica capillary 80 cm \times 75 μm)

As it is seen in Figure 7, all electropherograms can be divided into three regions: 1 – a positive relatively symmetrical sharp peak; 2 – a broad negative peak; 3 – a wide triangular-shape peak with the plateau at the end. As we also observed that HS without metal ions showed the electropherograms with flat baseline only, the formation of characteristic new peaks strongly suggests that these were evoked by the interaction of metal ions and HS. It may be suggested that two humps in the electropherograms – regions 1 and 3, indicate the formation of at least two different types of the Pb^{2+} and HS complexes. These complexes should have in total a negative charge (the HS at the pH 7 used in BGE have in total the negative charge) and are carried towards the cathode only because of the stronger EOF flow.

Due to the complexation of the molecules of free HS, their concentration drops in the reaction zone (region 2). The negative area of region 2 should express the vacancy of charged particles, which is formed by removing HS anions from the reaction zone in both direction – towards regions 1 and 3. This zone also moves along the capillary as a vacancy hump on the detector signal. The bulk EOF flow of the buffer is stronger than the movement of the complexes and it carries complexes and vacancy zones towards the cathode. The detector is placed near the cathodic end of the capillary and the recorded electropherogram appears in time as a mirror image of the real process.

5.4.1.2. Hypothetical model of the process occurring in the capillary

The hypothetical model of the processes occurring in the column filled with the HS solution after hydrodynamic injection of the zone of Pb^{2+} solution may be described as follows. As in a traditional EMMA process, the capillary is filled with the BGE solution – HS as Na-salt form – and the reactant (Pb^{2+}) is introduced into the capillary inlet as a separate band at the anodic end of the capillary (Figure 8A).

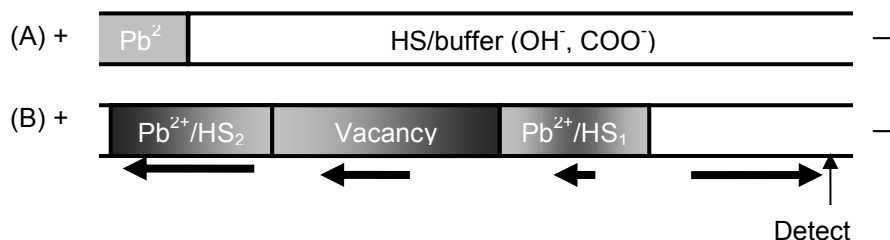


Figure 8. On-column reaction of Pb^{2+} and HS. (A) Filling of the capillary with HS fraction (pH=7) solution and metal solution injection; (B) Electrophoretic separation of the ions and migration of the products towards the detector after mixing of the analyte zone, the HS solution zone, and the reaction. Note that the shading of Pb^{2+}/HS zones approximately expresses the concentration distribution of complexes along the capillary. Arrows represent the value and direction of migration velocities of different reaction zones.

Upon application of an electric field, the two bands merge due to the differences in their electrophoretic mobilities. The positively charged Pb^{2+} ions having a positive electrophoretic mobility move rapidly toward the cathode (–) through the HS solution. The migration velocity of Pb^{2+} -ions and HS-anions is opposite under the selected conditions. The two zones mix, and the complexation reaction occurs. Simultaneously, the resultant products migrate away from the reaction zone and separate because electrophoretic mobilities of the products differ from the mobility of HS anions (Figure 8 B). Zones of complexes moving at different velocities, result in a complex electropherogram

signal. Thus, a detector can individually determine the relative amounts of different product [126].

5.4.1.3. Quantitative relationships of peak areas with added cation concentration

One can assume that, if the area of the specified region is quantitatively related to the concentration of the added metal, it should reflect the formation of the corresponding metal/HS complexes. Therefore, the peak area of regions 1, 2, and 3 was correlated with the concentration of added Pb^{2+} ions. The obtained results are presented in Table 7.

Table 7. The correlation of the peak areas of the regions 1, 2 and 3 with the concentration of the added $Pb(NO_3)_2$

Region	HS	Area				R^2	slope*
		Pb^{2+}	Pb^{2+}	Pb^{2+}	Pb^{2+}		
		$1 \cdot 10^{-4}$ M	$2 \cdot 10^{-4}$ M	$4 \cdot 10^{-4}$ M	$6 \cdot 10^{-4}$ M		
1	HA	1.22±0.10	1.53±0.17	3.05±0.52	4.50±0.09	0.9823	0.7628
	HMA	2.52±0.24	7.82±1.04	22.5±4.3	35.4±1.9	0.9731	5.6239
	FA	3.50±0.43	5.37±0.61	23.2±1.1	26.3±3.1	0.9313	4.6463
2	HA	-0.18±0.03	-0.60±0.06	-0.73±0.13	-0.63±0.11	0.5648	-0.1418
	HMA	-3.19±0.25	-7.75±1.09	-23.8±4.0	-40.0±5.7	0.9647	-6.2086
	FA	-4.26±0.59	-10.7±1.3	-30.7±1.8	-35.7±3.3	0.9588	-6.3625
3	HA	5.40±0.48	11.5±1.0	26.8±4.7	38.7±1.8	0.996	6.4526
	HMA	5.40±0.42	12.7±1.1	55.7±9.1	68.4±4.6	0.9398	11.649
	FA	7.02±0.76	14.4±1.4	32.0±2.0	39.3±2.5	0.9788	7.0109

* slope from the linear formula $y = mx$

Region 1. Region 1 that appears at the beginning in the electropherogram, can be associated with a complex, which is migrating by EOF towards the cathode (initially moving slowly towards the anode against EOF). The total migration time of the hump in region 1 decreases when the Pb^{2+} concentration increases, suggesting that the complex had been able to bind more metal ions and had become more positive. Thus, its overall velocity towards the cathode increases. For that region, a satisfactory good linear correlation of the peak area from the Pb^{2+} concentration was obtained for all HS fractions (HA, HMA and FA; $R^2 = 0.9823$; 0.9731 and 0.9313, correspondingly). The obtained correlation suggests that all HS fractions form similar metal/HS complexes (complex I). As expected for HS, the hump in region 1 is composed of several strongly overlapped peaks (Figure 7). These peaks may indicate the occurrence of several types of similar complexes, the value of velocity of which in the capillary is close. In the case of HMA and FA, the slope value of the linear correlation (Table 7) is several times larger than that for HA. That observation

may be connected with the different absorption coefficients of the formed complexes in the electric field. The largest peak area itself was observed for HMA and the smallest for HA. It means that, besides absorption differences, we also deal with the concentration of complex I in the capillary.

Region 3. Region 3 characterizes the migration of apparently the slowest migrating particles (the fastest towards the anode and slightly slower than EOF towards the cathode). In fact, it should be the complex with a higher charge to mass ratio than the free HS, because its movement consists of two components: one migrates to the anode and the other one moves to the opposite direction due to the bulk of EOF. HA and FA showed an excellent linear correlation with the concentration of inserted metal ($R^2 = 0.996$ and $R^2 = 0.9788$, respectively). It indicates that a second type of metal ion/HS complex (complex II) may exist. The HMA also reveals the existence of that complex, however, the correlation coefficient of the peak area from the inserted metal was somewhat lower ($R^2 = 0.9398$). The largest area values of the complex II had HMA, while HA and FA had almost the same area values. Thus, HA and FA may have almost the same amount of those functional groups that are related to the formation of complexes II.

Region 3 in Figure 7 has almost a triangular shape, which approaches nearly the constant level at higher metal concentration. The appearance of this hump may be explained as follows. If we assume that the equilibrium is substantially shifted towards the formation of complex II, then during the migration of the sample plug along the column, the amount of metal will be consumed by an irreversible process. Immediately after applying the high voltage, the available amount of the complexing sites on HS aggregates is limited (compared to the amount of metal ions), and the complex forming process has zero order resulting in the constant concentration of the complex II along the column. In a sufficient quantity of the sample has been consumed, the process turns to be the first order formation of complex II with a decreasing concentration along the column. The negatively charged particles migrate in the opposite direction relative to the EOF direction, as it was speculated above. Complex II moves faster against to the EOF than the complex I and, as a result, appears in the electropherograms later than complex I. Thus, the resulting shape of region 3 is a reflected image of concentration change in time at the detector window: the lowest concentration is seen first. Further, the concentration increases until saturation (change in the shape of the triangle).

It is known that HS form inner and outer sphere complexes. Outer sphere complexes form faster than inner sphere complexes. Outer sphere complexes may reflect the metal/HS complexes from region 1. Inner sphere complexes may be more hydrophobic. Pb^{2+} as the large and highly polarizable metal cation might prefer ligands that are more polarizable (e.g. S-, N- and P containing ligands) [95,97]. Therefore, complexes II may reflect inner sphere metal/HS complexes.

If regions 1 and 3 form the HS metal complexes, the sum of the areas must correlate linearly with the Pb^{2+} concentration. Indeed, the sum of areas of

regions 1 and 3 for each HS fraction has slightly better linear correlation with the injected Pb^{2+} concentration than the areas alone (Figure 9).

As it appears in Figure 9, each HS fraction has a different content of both metal/HS complexes. HMA has a higher content of both complexes than HA. Differences in the complexes must reflect the content of the corresponding functional groups in the HS fraction. As it can be seen, from all HS fractions, Pb^{2+} gives more complexes with HMA. Evidently, that fraction has more functional groups that are suitable for the Pb^{2+} complexation. Estimating from the slope value, HMA may have ~1.5 times more of both complexes than FA, and 2.4 times more than HA.

Region 2. Region 2 expresses the range of negative optical density compared to the HS-buffer solution. The negative area of region 2 should express the migration of the vacancy in the HS buffer of charged particles, i.e., by the absence of the HS particles that are consumed in the formation of the complexes I and II. The vacancy zone should migrate at the speed of the free HS anion. However, it is difficult to determine how regions 1 and 3 are related to region 2. The linear correlation of the area of region 2 with the injected Pb^{2+} concentration is worse than that of the other regions. The best linear correlations of the areas from the metal concentration had HMA and FA fractions ($R^2 = 0.9647$ and $R^2 = 0.9588$, respectively). HMA had the highest vacancy area values, which is apparently related to the highest values in regions 1 and 3. Taking into account the nature of the formation of region 2, one may conclude that region 2 is not suitable for the quantitative estimation of the concentration of metal/HS complexes.

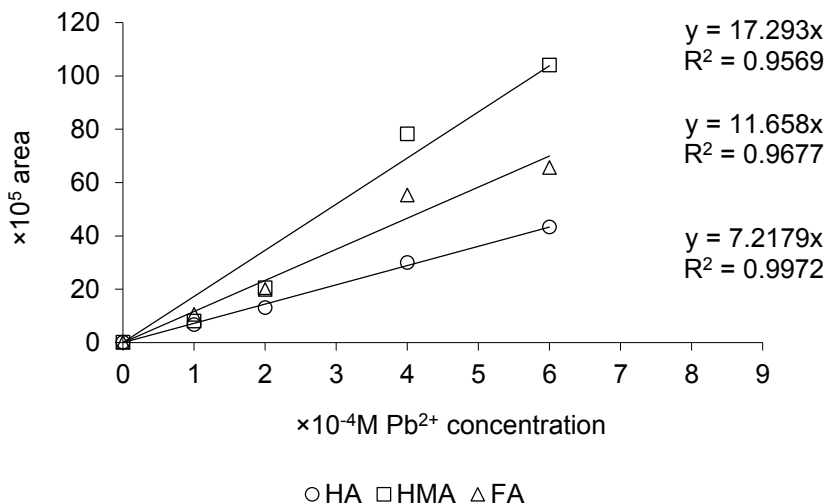


Figure 9. Dependence of the sum of areas in regions 1 and 3 for each HS fraction with injected Pb^{2+} concentration

5.4.1.4. Comparison of complexes I and II

From the literature data it is known that Pb^{2+} forms complexes with HS *via* two different kinds of binding sites: the strong and the weak binding sites. Weak binding sites include carboxyl and hydroxyl functional groups and strong binding sites (S-, N-, and P containing groups) form strong complexes with metals. Other authors also suggest formation of two kind complexes [90,95,97]. On the other hand, according to the general understanding of the EMMA process in capillary, symmetrical hump corresponds to the reversible ($A \leftrightarrow B$ type) process where the irreversible ($A \rightarrow B$ type) process results in the triangular hump. As it was explained above, the latter case can be explained by the continuous consumption of the reactant during its migration along the column and the decrease in the formation of the product, respectively (which manifests itself as a triangle on the electropherogram). Those considerations allow speculations about a possible nature of the complexes.

Reactions of HS with metal ions occur in two ways: as a major one, in which both carboxyl and phenolic hydroxyl groups participate simultaneously and as a minor one, which involves carboxyl groups only [92]. As the metal concentration is increased, the strong binding sites become saturated, and the excess metal then binds to the weaker sites, forming a labile weak complex [90]. In our case, region 1 may express the Pb^{2+} complexation with carbonyl and hydroxyl groups (complex I). Region 3 may express the metal complexation with more hydrophobic and polarizable structures giving complex II. As we can see in Table 7, region 3 (complex II) has always higher area values than region 1 (complex I). When calculating the ratio of the areas of regions 3 and 1 (Table 8) we found that for all HS fractions the ratio does not depend on the inserted Pb^{2+} concentration. However, each fraction has its own average value of the ratio. It may be suggested that in HMA and FA the amount of complex II is about two times higher than that of complex I. It may hint that in HA there are relatively more polarizable functional groups than in FA and HMA.

Table 8. Dependence of ratio of areas from regions 3 and 1 on the concentration of inserted Pb^{2+} -ions

Region 3/Region 1	$\times 10^{-4} M Pb^{2+}$ concentration				Average
	1	2	4	6	
HA	4.43	7.52	8.79	8.61	7.34 ± 1.45
HMA	2.11	1.28	2.47	1.93	1.95 ± 0.34
FA	2.01	2.68	1.38	1.49	1.89 ± 0.45

From all HS fractions HA had the highest molecular weight [7,13]. Our previous data showed that HA had more aliphatic structure than other HS fractions (Article I). The formation of inner sphere complexes may force the long carbon chains turn outside, thus making the Pb^{2+} /HA complex more hydrophobic. HA has less carboxylic structures than the other HS fractions

(Table 7), while HMA and FA have twice more hydrophobic and polarizable structures.

Comparing the elementary composition of HS fractions (Table 9, calculated from Article I) with the findings from electropherograms (Table 7), we may conclude that the amount of the complexes I is related to the content of the oxygen (connected mainly with the content of carboxyl and hydroxyl groups). Also, the relative amount of complex II that decreases in the order HMA>FA>HA is in good correlation with the values of the calculated aromaticity of those fractions (Table 9). The formation of complex II may also be connected with different binding sites that arise from groups other than carboxyl (nitrogen-, sulphur-, and oxygen-containing functional groups).

Table 9. Elementary composition and aromaticity of HS fractions

HS fractions	Ash, %	In HS fraction, %				Aromaticity, %
		C	H	N	O	
HA	33.0	33.7	5.0	4.8	23.4	13
HMA	11.8	47.6	6.0	2.6	32.0	35
FA	16.6	36.5	4.8	6.4	35.6	20

5.4.1.5. The rate of the formation of different complexes

Figure 7 shows that region 3 has a distinctive triangular shape. If we suggest that the shape of the region be connected with the formation of complexes II, the slope of that triangle should correspond to the rate of the formation of the complex. Based on that, we calculated the rate of the formation of the complex for all HS fractions from the initial slope at the beginning of region 3. We found that the obtained values (slope from Figure 7) do not correlate with the Pb^{2+} concentration in the case of HA and FA (Figure 10).

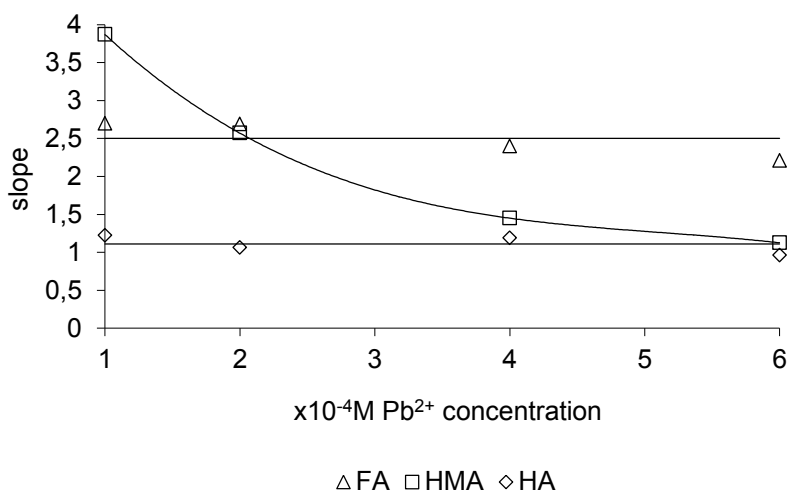


Figure 10. Dependence of the slope of region 3 and the Pb^{2+} concentration

It can be seen that HA and FA had different levels of slope values (1.11 ± 0.10 and 2.50 ± 0.19 , correspondingly). The formation of complex II is faster in FA fraction, probably because of the size of the particles: FA molecules are smaller than HA molecules [7,13]. In the case of HMA, the reaction rate depends on the metal concentration: an increase in the concentration of Pb^{2+} ions decreased the reaction rate. It may be related to the different types of processes that form the signal and that the slope does not express only the rate of the formation of complex II.

5.4.2. Interactions of Zn^{2+} with HA

The EMMA procedure was applied also to study the interaction of Zn^{2+} with HA. The introduction of ZnCl_2 to the HA column did not provide results similar to Pb^{2+} reproducible electropherograms. Instead, a relatively steady line with “spikes” appeared. The typical electropherograms recorded after injection of different concentration of Zn^{2+} solution are presented in Figure 11.

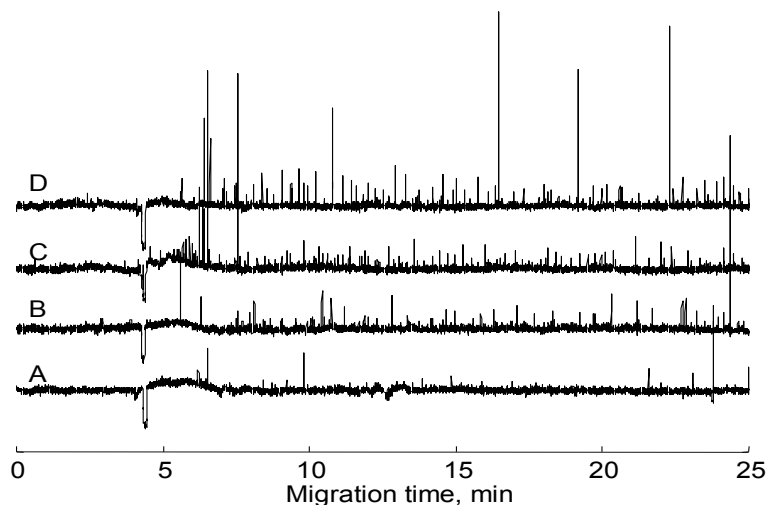


Figure 11. Electropherograms with HA as BGE (pH 7) at different concentrations of Zn^{2+} : A – $1 \cdot 10^{-4} \text{ M}$; B – $2 \cdot 10^{-4} \text{ M}$; C – $4 \cdot 10^{-4} \text{ M}$; D – $6 \cdot 10^{-4} \text{ M}$ (Separation voltage, 20 kV; hydrodynamic injection, 15 s; detection at 226 nm; fused-silica capillary 80 cm \times 75 μm)

The electropherograms show many randomly distributed small peaks (“spikes”). Their frequency depends on Zn^{2+} concentration. Measuring the mean number of those small peaks over a time span from 5 to 15 min (Figure 12), we found that their number had a linear correlation with inserted Zn^{2+} concentration ($R^2 = 0.9458$). We may conclude that we observe only the formation of different aggregate particles. HA as a colloidal solution can form aggregates at high voltage as we already demonstrated (Article III). Inserting metal ions to the HA

solution results in their colliding and clustering to the larger aggregates, that we observe as small peaks in electropherograms.

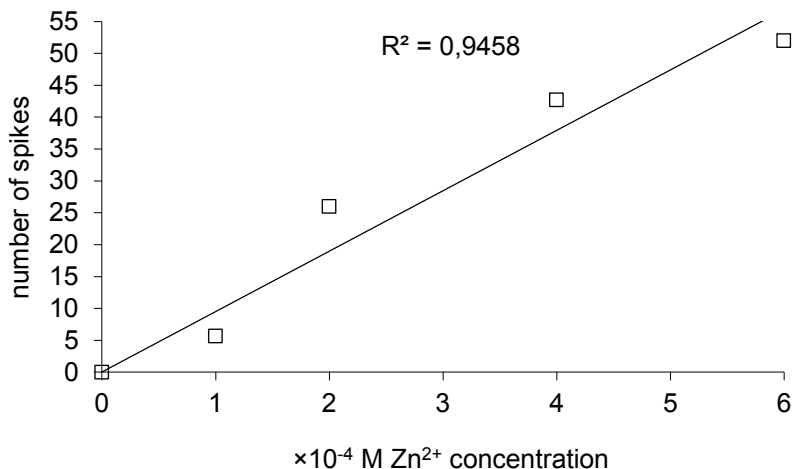


Figure 12. Number of spikes in HA electropherograms over a time span from 5 to 15 min in different Zn^{2+} concentrations

It is known from the literature data that Zn^{2+} complexes relatively weakly to HA [91] and prefers complexation with carboxyl groups [104,105]. From Pb^{2+} interaction with HA we know that HA fraction has 7.3 times more hydrophobic and polarizable groups than carboxyl and hydroxyl groups. Thus, we may conclude that HA does not have required quantity of Zn^{2+} complexation groups and, as the result of charge reduction by the cation aggregation occurs. From the precipitation experiment, we know that HA has the best precipitation ability with that metal. Thus, the Zn^{2+} /HA aggregates precipitated better than other Zn^{2+} /HS complexes (Article II). The appearance of “spikes” in electropherogram of HA with Zn^{2+} is in good agreement with these results.

CONCLUSIONS

- HS from the sediments from the Baltic Sea (Haapsalu Bay) and from the Lake Ermistu were characterized and compared by means of traditional physicochemical methods. For all HS fractions yield, elementary composition, initial content of metals and aromaticity was determined. It was found that metals concentrate differently to various HS fractions. According to these results, the stability order of initial metal/HS complexes is $\text{Cu} > \text{Zn} > \text{Mg} > \text{Fe}$.
- The HS fractions from the marine and the lake sediments differ slightly from each other in their ability to bind metal anions. The binding may cause flocculation, coagulation, and sedimentation of metal/HS complexes. The sedimentation of metal/HS complexes depends on the structure of HS fractions. From the sedimentation result, it was suggested that soluble carbohydrates cause the highest solubility of metal/FA complexes. HMA, on the other hand, contains more aromatic acids and phenols that are important in metal binding structures. Good precipitation of HA fractions is related to their aliphatic nature and use of non-dehydrated samples. The same precipitation order with cations: $\text{Pb}^{2+} > \text{Cu}^{2+} > \text{Zn}^{2+} > \text{Mn}^{2+} > \text{Mg}^{2+}$ was obtained for both, sea and lake HA fractions.
- The use of water-soluble HS as a background electrolyte in CE introduced by us offers new possibilities for the investigation of HS. We found that HA colloidal solution forms spikes in CE at high voltage. The formation of spikes in electropherograms depends on the applied voltage as well as on the concentration of the HA solutions.
- The nature of spikes in electropherograms was elucidated. It was demonstrated that spikes exhibit small new aggregates that form under the influence of high voltage electric field.
- We introduced the EMMA on-column approach in order to explore the complexation of metal ions with HS fraction and to follow the chemical reactions inside the capillary. From the obtained results we can suggest the structure differences in HS fractions:
 - HS fractions form two different types of complexes with Pb^{2+} cation, which have different mobilities in the electric field.
 - Complex I may express Pb^{2+} complexation with carbonyl and hydroxyl groups. Complex II may express complexation with relatively more polarizable functional groups.
 - HA contains mostly hydrophobic and polarizable groups, while HMA and FA have twice as many hydrophobic groups as carboxylic groups.
 - HA gives only aggregates with Zn^{2+} . Among other HS fractions with Zn^{2+} , HA has the best precipitation ability.

REFERENCES

1. Hayes, M. H. B. Humic substances: Progress towards more realistic concepts of structures. In G. Davis, E. A. Ghabbour (eds.) *Humic substances: structures, properties and uses*. – Royal Society of Chemistry, Cambridge, 1998, 1-28.
2. Cardellicchio, N., Palma, A., Montemurro, N., Ragone, P. Humic and fulvic acids in marine sediments in the Ionian Sea (Italy). In N. Senesi, T. M. Miano (eds.) *Humic substances in the global environment and implications for human health*. – Elsevier, Amsterdam, 1994, 819-824.
3. Novák, J., Kozler, J., Janoš, P., Čížiková, J., Tokarová, V., Madronová, L. Humic acids from coals of the North-Bohemian coal field I. Preparation and characterisation. – *React. Funct. Polym.* 2001, 47, 101-109.
4. Schmitt-Kopplin, P., Junkers, J. Capillary zone electrophoresis of natural organic matter. – *J. Chromatogr. A* 2003, 998, 1-20.
5. Schmitt, P., Kettrup, A., Freitag, D., Garrison, A. W. Flocculation of humic substances with metal ions as followed by capillary zone electrophoresis. – *Fresenius J. Anal. Chem.* 1996, 354, 915-920.
6. Von Wandruszka, R. Humic acids: Their detergent qualities and potential uses in pollution remediation. – *Geochem. Trans.* 2000, 1, 10-15.
7. Stevenson, F. J. Humus chemistry: genesis, composition, reactions, 2nd Edition. – John Wiley & Sons, New York, 1994.
8. Pokorná, L., Gajdošová, D., Mikeska, S., Havel, J. Analysis and characterization of a standard coal derived humic acid. In E. A. Ghabbour, G. Davies (eds.) *Humic Substances: Versatile Components of Plants, Soil and Water*. – Royal Society of Chemistry, Cambridge, 2000, 299-308.
9. Paciolla M. D., Davies, G., Jansen, S. A. Generation of hydroxyl radicals from metal-loaded humic acids. – *Environ. Sci. Technol.* 1999, 33, 1814-1818.
10. Klavinš, M. Aquatic humic substances: characterization, structure and genesis. – Riga, 1997.
11. Hayes, M. H. B. Emerging concepts of the compositions and structures of humic substances. In M. H. B. Hayes, W. S. Wilson (eds.) *Humic substances in soils, peats and waters. Health and environmental aspects*. – Royal Society of Chemistry, Cambridge, 1997, 3-30.
12. Piccolo, A., Conte, P., Cozzolino, A. Effects of mineral and monocarboxylic acids on the molecular association of dissolved humic substances. – *Eur. J. Soil Sci.* 1999, 50, 687-694.
13. Orlov, D. S. Soil humic acids and general humification theory. – Moskva, 1990. (In Russian).
14. Ilomets, T., Koorits, A., Peil, S., Pärn, A., Salm, S., Utsal, K., Utsal, V., Veermäe, I. A comparative study of Estonian curative muds. – *Acta Comm. Univ. Tartuensis, Publ. Chem. XXI* 1993, 214-229.
15. Takács, M. Cu(II) and Pb(II) complexation by humic and fulvic acids: conditional stability constants and their correlation with humus quality. In

- N. Senesi, T. M. Miano (eds) *Humic substances in the global environment and implications for human health*. – Elsevier, Amsterdam, 1994, 475-480.
16. Abate, M., Masini, J. C. Acid-basic and complexation properties of a sedimentary humic acid. A study on the Barra Bonita Reservoir of Tietê River, São Paulo State, Brazil. – *J Braz. Chem. Soc.* 2001, 12, 109-116.
 17. Jurcsik, I. Investigation in the mechanism of electron transmission and active oxygen generating humic acids supported by redoxindicator. In N. Senesi, T. M. Miano (eds) *Humic substances in the global environment and implications for human health*. – Elsevier, Amsterdam, 1994, 311-316.
 18. Glebova, G. I. Hymatomelanic acids in soils. Moskva, 1985. (In Russian).
 19. Koivula, N., Hänninen, K. Concentrations of monosaccharides in humic substances in the early stages of humification. – *Chemosphere* 2001, 44, 271-279.
 20. Cheshire, M. V. Origins and stability of soil polysaccharide. – *J. Soil Sci.* 1977, 28, 1-10.
 21. Schnitzer, M. A. Chemical structure for humic acid. Chemical, ¹³C NMR, colloid chemical, and electron microscopic evidence. In N. Senesi, T. M. Miano (eds.) *Humic substances in the global environment and implications for human health*. – Elsevier, Amsterdam, 1994, 57-69.
 22. Fetsch, D., Hradilová, M., Peña Méndez, E. M., Havel, J. Capillary zone electrophoresis study of aggregation of humic substances. – *J. Chromatogr. A* 1998, 817, 313-323.
 23. Pacheco, M. L., Peña-Méndez, E. M., Havel, J. Supramolecular interactions of humic acids with organic and inorganic xenobiotics studied by capillary electrophoresis. – *Chemosphere* 2003, 51, 95-108.
 24. Fetsch, D., Havel, J. Capillary zone electrophoresis for the separation and characterization of humic acids. – *J. Chromatogr. A* 1998, 802, 189-202.
 25. Young, C., von Wandruszka, R. A comparison of aggregation behavior in aqueous humic acids. – *Geochem. Trans.* 2001, 2, 16-20.
 26. Riggle, J., von Wandruszka, R. Dynamic conductivity measurements in humic and fulvic acid solutions. – *Talanta* 2004, 62, 103-108.
 27. Von Wandruszka, R., Engebretson, R. R., Yates III, L. M. Humic acid pseudomicelles in dilute aqueous solution: fluorescence and surface tension measurements. In E. A. Ghabbour, G. Davies (eds) *Understanding humic substances: advanced methods, properties and applications*. – Royal Society of Chemistry, Cambridge, 1999, 79-85.
 28. Janoš, P. Separation methods in the chemistry of humic substances. – *J. Chromatogr. A* 2003, 983, 1-18.
 29. Li, L., Zhao, Z., Huang, W., Peng, P., Sheng, G., Fu, J. Characterization of humic acids fractionated by ultrafiltration. – *Org. Geochem.* 2004, 35, 1025-1037.
 30. Assemi, S., Newcombe, G., Hepplewhite, C., Beckett, R. Characterization of natural organic matter fractions separated by ultrafiltration using flow field-flow fractionation. – *Water Res.* 2004, 38, 1467-1476.

31. Hafidi, M., Amir, S., Revel, J.-C. Structural characterization of olive mill waster-water after aerobic digestion using elemental analysis, FTIR and ¹³C NMR. – *Process Biochemistry* 2004, In Press, online 19 August 2004.
32. Baddi, G. A., Hafidi, M., Cegarra, J., Alburquerque, J. A., González, J., Gilard, V., Revel, J.-C. Characterization of fulvic acids by elemental and spectroscopic (FTIR and ¹³C-NMR) analyses during composting of olive mill wastes plus straw. – *Bioresource Technol.* 2004, 93, 285-290.
33. Wang, M. C., Liu, C. P., Sheu, B. H. Characterization of organic matter in rainfall, throughfall, stemflow, and streamwater from three subtropical forest ecosystems. – *J. Hydrol.* 2004, 289, 275-285.
34. Thomsen, M., Lassen, P., Dobel, S., Hansen, P.E., Carlsen, L., Mogensen, B. B. Characterisation of humic materials of different origin: A multivariate approach for quantifying the latent properties of dissolved organic matter. – *Chemosphere* 2002, 49, 1327-1337.
35. Pérez, M. G., Martin-Neto, L., Saab, S. C., Novotny, E. H., Milori, D. M. B. P., Bagnato, V. S., Colnago, L. A., Melo, W. J., Knicker, H. Characterization of humic acids from a Brazilian Oxisol under different tillage systems by EPR, ¹³C NMR, FTIR and fluorescence spectroscopy. – *Geoderma* 2004, 118, 181-190.
36. Claret, F., Schäfer, T., Bauer, A., Buckau, G. Generation of humic and fulvic acid from Callovo-Oxfordian clay under high alkaline conditions. – *Sci. Total Environ.* 2003, 317, 189-200.
37. Kang, K. H., Shin, H. S., Park, H. Characterization of humic substances present in landfill leachates with different landfill ages and its implications. – *Water Res.* 2002, 36, 4023-4032.
38. Chen, J., Gu, B., LeBoeuf, E. J., Pan, H., Dai, S. Spectroscopic characterization of the structural and functional properties of natural organic matter fractions. – *Chemosphere* 2002, 48, 59-68.
39. Ussiri, D. A. N., Johnson, C.E. Characterization of organic matter in a northern hardwood forest soil by ¹³C NMR spectroscopy and chemical methods. – *Geoderma* 2003, 111, 123-149.
40. Monteil-Rivera, F., Brouwer, E. B., Masset, S., Deslandes, Y., Dumonceau, J. Combination of X-ray photoelectron and solid-state ¹³C nuclear magnetic resonance spectroscopy in the structural characterisation of humic acids. – *Anal. Chim. Acta* 2000, 424, 243-255.
41. Tao, Z.-Y., Zhang, J., Zhai, J.-J. Characterization and differentiation of humic acids and fulvic acids in soils from various regions of China by nuclear magnetic resonance spectroscopy. – *Anal. Chim. Acta* 1999, 395, 199-203.
42. Hoque, E., Wolf, M., Teichmann, G., Peller, E., Schimmack, W., Buckau, G. Influence of ionic strength and organic modifier concentrations on characterization of aquatic fulvic and humic acids by high-performance size-exclusion chromatography. – *J. Chromatogr. A* 2003, 1017, 97-105.
43. Nagao, S., Matsunaga, T., Suzuki, Y., Ueno, T., Amano, H. Characteristics of humic substances in the Kuji River waters as determined by high-

- performance size exclusion chromatography with fluorescence detection. – *Water Res.* 2003, 37, 4159-4170.
44. von Wandruszka, R., Schimpf, M., Hill, M., Engebretson, R. Characterization of humic acid size fractions by SEC and MALS. – *Org. Geochem.* 1999, 30, 229-235.
 45. Jaffé, R., Boyer, J. N., Lu, X., Maie, N., Yang, C., Scully, N. M., Mock, S. Source characterization of dissolved organic matter in a subtropical mangrove-dominated estuary by fluorescence analysis. – *Mar. Chem.* 2004, 84, 195-210.
 46. Peuravuori, J., Koivikko, R., Pihlaja, K. Characterization, differentiation and classification of aquatic humic matter separated with different sorbents: synchronous scanning fluorescence spectroscopy. – *Water Res.* 2002, 36, 4552-4562.
 47. Song, X., Farwell, S. O. Pyrolysis gas chromatography atomic emission detection method for determination of N-containing components of humic and fulvic acids. – *J. Anal. Appl. Pyrol.* 2004, 71, 901-915.
 48. Olivella, M. A., del Río, J. C., Palacios, J., Vairavamurthy, M. A., de las Heras, F. X. C. Characterization of humic acid from leonardite coal: an integrated study of PY-GC-MS, XPS and XANES techniques. – *J. Anal. Appl. Pyrol.* 2002, 63, 59-68.
 49. Mansuy, L., Bourezgui, Y., Garnier-Zarli, E., Jardé, E., Réveillé, V. Characterization of humic substances in highly polluted river sediments by pyrolysis methylation–gas chromatography–mass spectrometry. – *Org. Geochem.* 2001, 32, 223-231.
 50. Hutta, M., Góra, R. Novel stepwise gradient reversed-phase liquid chromatography separations of humic substances, air particulate humic-like substances and lignins. – *J. Chromatogr. A* 2003, 1012, 67-79.
 51. Wu, F. C., Evans, R. D., Dillon, P. J. High-performance liquid chromatographic fractionation and characterization of fulvic acid. – *Anal. Chim. Acta* 2002, 464, 47-55.
 52. Kujawinski, E. B., Freitas, M. A., Zang, X., Hatcher, P. G., Green-Church, K. B., Jones, R. B. The application of electrospray ionization mass spectrometry (ESI MS) to the structural characterization of natural organic matter. – *Org. Geochem.* 2002, 33, 171-180.
 53. Pfeifer, T., Klaus, U., Hoffmann, R., Spiteller, M. Characterisation of humic substances using atmospheric pressure chemical ionisation and electrospray ionisation mass spectrometry combined with size-exclusion chromatography. – *J. Chromatogr. A* 2001, 926, 151-159.
 54. Riggle, J., von Wandruszka, R. Conductometric characterization of dissolved humic materials. – *Talanta* 2002, 57, 519-526.
 55. Dunkelog, R., Rüttinger, H.-H., Peisker, K. Comparative study for the separation of aquatic humic substances by electrophoresis. – *J. Chromatogr. A* 1997, 777, 355-362.

56. Schmitt-Kopplin, Ph., Garrison, A. W., Perdue, E. M., Freitag, D., Kettrup. Capillary electrophoresis in the analysis of humic substances. Facts and artifacts. – *J. Chromatogr. A* 1998, 807, 101-109.
57. Pokorná, L., Pacheco, M. L., Havel J. Highly reproducible capillary zone electrophoresis of humic acids in cyclodextrin- or oligosaccharide-modified background electrolytes. – *J. Chromatogr. A* 2000, 895, 345-350.
58. Pompe, S., Heise, K.-H., Nitsche, H. Capillary electrophoresis for a “finger-print” characterization of fulvic and humic acids. – *J. Chromatogr. A* 1996, 723, 215-218.
59. Peuravuori, J., Lepane, V., Lehtonen, T., Pihlaja, K. Comparative study for separation of aquatic humic substances by capillary zone electrophoresis using uncoated, polymer coated and gel-filled capillaries. – *J Chromatogr. A* 2004, 1023, 129-142.
60. Gajdošová, D., Novotná, K., Prošek, P., Havel, J. Separation and characterization of humic acids from Antarctica by capillary electrophoresis and matrix-assisted laser desorption ionization time-of-flight mass spectrometry: Inclusion complexes of humic acids with cyclodextrins. – *J. Chromatogr. A* 2003, 1014, 117-127.
61. Cavani, L., Ciavatta, C., Trubetskaya, O. E., Reznikova, O. I., Afanas'eva, G. V., Trubetskoj, O. A. Capillary zone electrophoresis of soil humic acid fractions obtained by coupling size-exclusion chromatography and polyacrylamide gel electrophoresis. – *J. Chromatogr. A* 2003, 983, 263-270.
62. Larsen, K. L., Zimmermann, W. Analysis and characterization of cyclodextrins and their inclusion complexes by affinity capillary electrophoresis. – *J. Chromatogr. A*, 1999, 836, 3-14.
63. Schmitt-Kopplin, P., Freitag, D., Kettrup, A., Schoen, U., Egeberg, P. Kr. Capillary zone electrophoretic studies on Norwegian surface water natural organic matter. – *Environ. Int.* 1999, 25, 259-274.
64. Lepane, V. Comparison of XAD resins for the isolation of humic substances from seawater. – *J. Chromatogr. A* 1999, 845, 329-335.
65. Egeberg, P. Kr., Bergli, S. O. Fingerprinting of natural organic matter by capillary zone electrophoresis using organic modifiers and pattern recognition analysis. – *J. Chromatogr. A* 2002, 950, 221-231.
66. Schmitt, Ph., Freitag, D., Trapp, I., Garrison, A. W., Schiavon, M., Kettrup, A. Binding of s-triazines to dissolved humic substances: Electrophoretic approaches using Affinity Capillary Electrophoresis (ACE) and Micellar Electrokinetic Chromatography (MEKC). – *Chemosphere* 1997, 35, 55-75.
67. Pacheco, M. L., Havel, J. Capillary zone electrophoresis of humic acids from the American continent. – *Electrophoresis* 2002, 23, 268-277.
68. He, L., Jepsen, R. J., Evans, L. E., Armstrong, D. W. Electrophoretic Behavior and Potency Assessment of Boar Sperm Using a Capillary Electrophoresis-Laser Induced Fluorescence System. – *Anal. Chem.* 2003, 75, 825-834.

69. Zheng, J., Yeung, E. S. Mechanism of Microbial Aggregation during Capillary Electrophoresis. – *Anal. Chem.* 2003, 75, 818-824.
70. Tokalioğlu, Ş., Kartal, Ş., Latif, E. Speciation and determination of heavy metals in lake waters by atomic absorption spectrometry after sorption on Amberlite XAD-16 resin. – *Anal. Sci.* 2000, 16, 1169-1174.
71. Cook, R. L., Langford, C. H. A biogeopolymeric view of humic substances with application to paramagnetic metal effects on ¹³C NMR. In E. A. Ghabbour, G. Davies (eds.) *Understanding humic substances: advanced methods, properties and applications*. – The Royal Society of Chemistry, Cambridge, 1999, 31-48.
72. Lubal, P., Fetsch, D., Šíroký, D., Lubalová, M., Šenkýr, J., Havel, J. Potentiometric and spectroscopic study of uranyl complexation with humic acids. – *Talanta* 2000, 51, 977-991.
73. Marx, G., Heumann, K. G. Mass spectrometric investigations of the kinetic stability of chromium and copper complexes with humic substances by isotope-labelling experiments. – *Fresenius J. Anal. Chem.* 1999, 364, 489-494.
74. Koczorowska, E., Slawinski, J. Model studies of zinc bonding with humic acid in the presence of UV-VIS-NIR radiation. – *Chemosphere* 2003, 51, 693-700.
75. Jerzykiewicz, M., Jezierski, A., Czechowski, F., Drozd, J. Influence of metal ions binding on free radical concentration in humic acids. A quantitative electron paramagnetic resonance study. – *Org. Geochem.* 2002, 33, 265-268.
76. Ruiz-Haas, P., Amarasiriwardena, D., Xing, B. Determination of trace metals bound to soil humic acid species by size exclusion chromatography and inductively coupled plasma mass spectrometry. In G. Davis, E. A. Ghabbour (eds) *Humic substances: structures, properties and uses*. – Royal Society of Chemistry, Cambridge, 1998, 147-163.
77. Nórden, M., Dabek-Zlotorzynska, E. Study of metal-fulvic acid interactions by capillary electrophoresis. – *J. Chromatogr. A* 1996, 739, 421-429.
78. Lubal, P., Šíroký, D., Fetsch, D., Havel, J. The acidobasic and complexation properties of humic acids. Study of complexation of Czech humic acids with metal ions. – *Talanta* 1998, 47, 401-412.
79. Kam, S. K., Gregory, J. The interaction of humic substances with cationic polyelectrolytes. – *Wat. Res.* 2001, 35, 3557-3566.
80. Impellitteri, C. A., Lu, Y., Saxe, J. K., Allen, H. E., Peijnenburg, W. J. G. M. Correlation of the partitioning of dissolved organic matter fractions with the desorption of Cd, Cu, Ni, Pb and Zn from 18 Dutch soils. – *Environ. Int.* 2002, 28, 401-410.
81. Martyniuk, H., Więckowska, J. Adsorption of metal ions on humic acids extracted from brown coals. – *Fuel Process. Technol.* 2003, 84, 23-36.
82. Wall, N. A., Choppin, G. R. Humic acids coagulation: influence of divalent cations. – *Appl. Geochim.* 2003, 18, 1573-1582.

83. Kurková, M., Klika, Z., Kliková, C., Havel, J. Humic acids from oxidized coals. I. Elemental composition, titration curves, heavy metals in HA samples, nuclear magnetic resonance spectra of HAs and infrared spectroscopy. – *Chemosphere* 2004, 54, 1237-1245.
84. Von Wandruszka, R., Ragle, C., Engebretson, R. The role of selected cations in the formation of pseudomicelles in aqueous humic acid. – *Talanta* 1997, 44, 805-809.
85. Gaffney, J. S., Marley, N. A., Clark, S. B. Humic and fulvic acids and organic colloidal materials in the environment. In J. S. Gaffney, N. A. Marley, S. B. Clark (eds.) *Humic and fulvic acids: isolation, structure and environmental role*. – American Chemical Society, Washington DC, 1996, 2-16.
86. Bryan, N. D., Jones, M. N., Birkett, J., Livens, F. R. Aggregation of humic substances by metal ions measured by ultracentrifugation. – *Anal. Chim. Acta* 2001, 437, 291-308.
87. Evangelou, V. P., Marsi, M., Chappell, M. A. Potentiometric-spectroscopic evaluation of metal-ion complexes by humic fractions extracted from corn tissue. – *Spectrochim. Acta A* 2002, 58, 2159-2175.
88. Guéguen, C., Koukal, B., Dominik, J., Pardos, M. Competition between alga (*Pseudokirchneriella subcapitata*), humic substances and EDTA for Cd and Zn control in the algal assay procedure (AAP) medium. – *Chemosphere* 2003, 53, 927-934.
89. Čížiková, J., Kozler, J., Madronová, L., Novák, J., Janoš, P. Humic acids from coals of the North-Bohemian coal field II. Metal-binding capacity under static conditions. – *React. Funct. Polym.* 2001, 47, 111-118.
90. Sekaly, A. L. R., Mandal, R., Hassan, N. M., Murimboh, J., Chakrabarti, C. L., Back, M. H., Grégoire, D. C., Schroeder, W. H. Effect of metal/fulvic acid mole ratios on the binding of Ni(II), Pb(II), Cu(II), Cd(II), and Al(III) by two well-characterized fulvic acids in aqueous model solutions. – *Anal. Chim. Acta* 1999, 402, 211-221.
91. Livens, F. R. Chemical reactions of metals with humic material. – *Eviron. Pollut.* 1991, 70, 183-208.
92. Pandey, A. K., Pandey, S. D., Misra, V. Stability constants of metal-humic acid complexes and its role in environmental detoxification. – *Ecotox. Environ. Safe.* 2000, 47, 195-200.
93. Madronová, I., Kozler, J., Čížiková, J., Novák, J., Janoš, P. Humic acids from coal of the North-Bohemia coal field III. Metal-binding properties of humic acids – measurements in a column arrangement. – *React. Funct. Polym.* 2001, 47, 119-123.
94. Esteves da Silva, J. C. G., Oliveira, C. J. S. Metal ion complexation properties of fulvic acids extracted from composted sewage sludge as compared to a soil fulvic acid. – *Water Res.* 2002, 36, 3404-3409.
95. Logan, E. M., Pulford, I. D., Cook, G. T., Mackenzie, A. B. Complexation of Cu²⁺ and Pb²⁺ by peat and humic acid. – *Eur. J. Soil Sci.* 1997, 48, 685-696.

96. Saar, R. A., Weber, J. H. Lead(II) complexation by fulvic acid: how it differs from fulvic acid complexation of copper(II) and cadmium(II). – *Geochim. Cosmochim. Ac.* 1980, 44, 1381-1384.
97. Xia, K., Bleam, W., Helmke, P. A. Studies of the nature of Cu²⁺ and Pb²⁺ binding sites in soil humic substances using X-ray absorption spectroscopy. – *Geochim. Cosmochim. Ac.* 1997, 61, 2211-2221.
98. Alvarez-Puebla, R. A., Valenzuela-Calahorro, C., Garrido, J. J. Cu(II) retention on a humic substance. – *J. Colloid Interf. Sci.* 2004, 270, 47-55.
99. Abate, G., Masini, J. C. Complexation of Cd(II) and Pb(II) with humic acids studied by anodic stripping voltammetry using differential equilibrium functions and discrete site models. – *Org. Geochem.* 2002, 33, 1171-1182.
100. Christl, I., Milne, C. J., Kinniburgh, D. G., Kretzschmar, R. Relating ion binding by fulvic and humic acids to chemical composition and molecular size. 2. Metal binding. – *Environ. Sci. Technol.* 2001, 35, 2512-2517.
101. Pacheco, M. L., Havel, J. Capillary zone electrophoretic (CZE) study of uranium(VI) complexation with humic acids. – *J. Radioanal. Nucl. Chem.* 2001, 248, 565-570.
102. Jerzykiewicz, M. Formation of new radicals in humic acids upon interaction Pb(II) ions. – *Geoderma* 2004, 122, 305-309.
103. Nantsis, E. A., Carper, W. R. Molecular structure of divalent metal ion-fulvic acid complexes. – *J. Mol. Struc.-Theochem* 1998, 423, 203-212.
104. Nakayama, M., Fujiyoshi, R., Sawamura, S. Humic acids as a scavenger of manganese(II) and zinc(II) in soil environment using a radiotracer technique. – *J. Radioanal. Nucl. Ch.* 2001, 250, 433-436.
105. Xia, K., Bleam, W., Helmke, P. A. Studies of the nature of binding sites of first row transition elements bound to aquatic and soil humic substances using X-ray absorption spectroscopy. – *Geochim. Cosmochim. Ac.* 1997, 61, 2223-2235.
106. Jones, M. N., Bryan, N. D. Colloidal properties of humic substances. – *Adv. Colloid Interfac.* 1998, 78, 1-48.
107. Piana, M. J., Zahir, K. O. Investigation of metal ions binding of humic substances using fluorescence emission and synchronous-scan spectroscopy. – *J. Environ. Sci. Health B* 2000, 35, 87-102.
108. van Leeuwen, H. P., Town, R. M. Stripping chronopotentiometry for metal ion speciation analysis at a microelectrode. – *J. Electroanal. Chem.* 2002, 523, 16-25.
109. van Staden, J. J., van den Hoop, M. A. G. T., Cleven, R. F. M. J. Characterization of metal/humic acid systems by Capillary Electrophoresis.
<http://www.rivm.nl/bibliotheek/rapporten/518001007.html>
110. Nifant'jeva, T. I., Burba, P., Fedorova, O., Shkinev, V. M., Spivakov, B. Ya. Ultrafiltration and determination of Zn- and Cu-humic substances complexes stability constants. – *Talanta* 2001, 53, 1127-1131.

111. Tipping, E., Rieuwerts, J., Pan, G., Ashmore, M. R., Lofts, S., Hill, M. T. R., Farago, M. E., Thornton, I. The solid–solution partitioning of heavy metals (Cu, Zn, Cd, Pb) in upland soils of England and Wales. – *Environ. Pollut.* 2003, 125, 213-225.
112. Plachke, M., Rothe, J., Denecke, M. A., Fanghänel T. Soft X-ray spectromicroscopy of humic acid europium(III) complexation by comparison to model substances. – *J. Electron Spectrosc.* 2004, 135, 55-64.
113. Donisa, C., Mocanu, R., Steinnes, E. Distribution of some major and minor elements between fulvic and humic fractions in natural soils. – *Geoderma* 2003, 111, 75-84.
114. Filella, M., Town, R. M. Determination of metal ion binding parameters for humic substances: Part 1. Application of a simple calculation method for extraction of meaningful parameters from reverse pulse polarograms. – *J. Electroanal. Chem.* 2000, 485, 21-33.
115. Town, R. M., Filella, M. Determination of metal ion binding parameters for humic substances: Part 2. Utility of ASV pseudo-polarography. – *J. Electroanal. Chem.* 2000, 488, 1-16.
116. Shi, Y., Fritz, J. S. Separation of metal ions by capillary electrophoresis with a complexing electrolyte. – *J. Chromatogr.* 1993, 640, 473-479.
117. Regan, F. B., Meaney, M. P., Lunte, S. M. Determination of metal ions by capillary electrophoresis using on-column complexation with 4-(2-pyridylazo)resorcinol following trace enrichment by peak stacking. – *J. Chromatogr. B* 1994, 657, 409-417.
118. Haumann, I., Bächmann, K. On-column chelation of metal ions in capillary zone electrophoresis. – *J. Chromatogr. A* 1995, 717, 385-391.
119. Padaruskas, A., Schwedt, G. Capillary electrophoresis in metal analysis: Investigations of multi-elemental separation of metal chelates with aminopolycarboxylic acids. – *J. Chromatogr. A* 1997, 773, 351-360.
120. Dabek-Zlotorzynska, E., Lai, E. P. C., Timberbaev, A. R. Capillary electrophoresis: the state-of-the-art in metal speciation studies. – *Anal. Chim. Acta.* 1998, 359, 1-26.
121. Chen, Z.-L., Naidu, R. On-column complexation of metal ions using 2,6-pyridinedicarboxylic acid and separation of their anionic complexes by capillary electrophoresis with direct UV detection. – *J. Chromatogr. A* 2002, 966, 245-251.
122. Wang, M., Lin, J. M., Qu, F., Shan, X., Chen, Z. On-capillary complexation of metal ions with 4-(2-thiazolylazo)resorcinol in capillary electrophoresis. – *J. Chromatogr. A* 2004, 1029, 249-254.
123. Naujalis, E., Padaruskas, A. Development of capillary electrophoresis for the determination of metal ions using mixed partial and complete complexation techniques. – *J. Chromatogr. A* 2002, 977, 135-142.
124. Liu, B. F., Liu, L. B., Cheng, J. K. Analysis of metal complexes in the presence of mixed ion pairing additives in capillary electrophoresis. – *J. Chromatogr. A* 1999, 848, 473-484.

125. Chen, Z., Naidu, R., Subramanian, A. Separation of chromium (III) and chromium (VI) by capillary electrophoresis using 2,6-pyridinedicarboxylic acid as a pre-column complexation agent. – *J. Chromatogr. A* 2001, 927, 219-227.
126. Bao, J., Regnier, F. E. Ultramicro enzyme assays in a capillary electrophoretic system. – *J. Chromatogr.* 1992, 608, 217-224.
127. Saevels, J., Van Schepdael, A., Hoogmartens, J. Determination of the kinetic parameters of adenosine deaminase by electrophoresis mediated microanalysis. – *Electrophoresis* 1996, 17, 1222-1227.
128. Kwak, E. S., Esquivel, S., Gomez, F. A. Optimization of capillary electrophoresis conditions for in-capillary enzyme-catalyzed microreactions. – *Anal. Chim. Acta* 1999, 397, 183-190.
129. Nováková, S., Glatz, Z. Determination of the kinetic parameters of rhodanese by electrophoretically mediated microanalysis in a partially filled capillary. – *Electrophoresis* 2002, 23, 1063-1069.
130. Van Dyck, S., Kaale, E., Nováková, S., Glatz, Z., Hoogmartens, J., Van Schepdael, A. Advances in capillary electrophoretically mediated microanalysis. – *Electrophoresis* 2003, 24, 3868-3878.
131. Nováková, S., Van Dyck, S., Van Schepdael, A., Hoogmartens, J., Glatz, Z. Electrophoretically mediated microanalysis. – *J. Chromatogr. A* 2004, 1032, 173-184.
132. Yamashiro, T., Okada, T. Capillary electrophoresis as a nanoreactor of separation capability: on-capillary reaction catalyzed by transition metal ions. – *Electrophoresis* 2003, 24, 2168-2173.
133. Andreev, V. P., Ilyina, N. B., Lebedeva, E. V., Kamenev, A. G., Popov, N. S. Electroinjection analysis. Concept, mathematical model and applications. – *J. Chromatogr. A* 1997, 772, 115-127.
134. Goh, K. M., Reid, M. R. Molecular weight distribution of soil organic matter as affected by acid pre-treatment and fractionation into humic and fulvic acids. – *J. Soil Sci.* 1975, 26, 207-222.
135. Abbt-Braun, G., Lankes, U., Frimmel, F. H. Structural characterization of aquatic humic substances – The need for a multiple method approach. – *Aquat. Sci.* 2004, 66, 151-170.
136. Belzile, N., Joly, H. A., Li, H. Characterization of humic substances extracted from Canadian lake sediments. – *Can. J. Chem.* 1997, 75, 14-27.
137. Ishiwatari, R. Geochemistry of humic substances in lake sediments. In G. R. Aiken, D. M. McKnight, R. L. Wershaw, P. Maccarthy (eds.) *Humic substances in soil, sediment and water geochemistry, isolation and characterization*. – John Wiley & Sons, New York, 1985, 147-180.
138. Peuravuori, J., Pihlaja, K. Molecular size distribution and spectroscopic properties of aquatic humic substances. – *Anal. Chim. Acta* 1997, 337, 133-149.
139. Chin, Y. P., Aiken, G., O'Loughlin, E. Molecular weight, polydispersity and spectroscopic properties of aquatic humic substances. – *Environ. Sci. Technol.* 1994, 28, 1853-1858.

140. Klavinš, M., Seržāne, J., Supe, A. Properties of soil and peat humic substances from Latvia. – *Proc. Latvian Acad. Sci. B* 1999, 53, 249-255.
141. Soga, T., Ross, G. A., Simultaneous determination of inorganic anions, organic acids and metal cations by capillary electrophoresis. – *J. Chromatogr. A* 1999, 834, 65-71.
142. Baraj, B., Martinez, M., Sastre, A., Aguilar, M. Simultaneous determination of Cr(III), Fe(III), Cu(II) and Pb(II) as UV-absorbing EDTA complexes by capillary zone electrophoresis. – *J. Chromatogr. A* 1995, 695, 103-111.
143. Hinsmann, P., Arce, L., Valcárcel, A. R. M. Determination of pesticides in waters by automatic on-line solid-phase extraction–capillary electrophoresis. – *J. Chromatogr. A* 2000, 866, 137-146.
144. Lee, Y.-H., Lin, T.-I. Determination of metal cations by capillary electrophoresis effect of background carrier and completing agents. – *J. Chromatogr. A* 1994, 675, 227-236.
145. Lemaire, E., Merhi, D., Pérez, A. T., Valverde, J. M. Mechanical stresses of a layer of colloidal particles aggregated by means of an electric field. – *J. Electrostatics* 2001, 53, 107-121.
146. Radko, S. P., Chrambach, A. Separation and characterization of sub- μm - and μm -sized particles by capillary zone electrophoresis. – *Electrophoresis* 2002, 23, 1957-1972.
147. Petersen, S. L., Ballou, N. E. Separation of micrometer-size oxide particles by capillary zone electrophoresis. – *J. Chromatogr. A* 1999, 834, 445-452.

ACKNOWLEDGEMENTS

This work was conducted in the Department of Chemistry of the Faculty of Science at Tallinn University of Technology.

I am very grateful to my supervisor Margus Lopp for his patience and for giving me excellent support and inspiration that I needed.

I am grateful to my colleagues and co-authors: Merike Vaher, Marina Kudrjashova, Viia Lepane, Maili Treumann, Anu Viitak and Kati Helmja for their excellent collaboration and all kind of help during these years.

I thank Mihkel Kaljurand for his support during these years and for explaining the nature of capillary electrophoresis.

My special thanks are due to Tullio Ilomets and Robert Trink for sharing their knowledge about humic substances in Estonian sediments.

In addition, I would like to thank my family and parents for their support during all these years.